AGRICULTURAL UNIVERSITY OF ATHENS
SCHOOL OF APPLIED BIOLOGY & BIOTECHNOLOGY
DEPARTMENT OF BIOTECHNOLOGY

MASTER'S PROGRAMME IN SYSTEMS BIOLOGY

Master Thesis

Computational drug repurposing in Claudin-low breast cancer subtype

Ioannis S. Kontos

Supervisor:
Thireou Trias, Assistant Professor, Agricultural University of Athens

ATHENS
2024

AGRICULTURAL UNIVERSITY OF ATHENS
SCHOOL OF APPLIED BIOLOGY & BIOTECHNOLOGY
DEPARTMENT OF BIOTECHNOLOGY

Master Thesis

Computational drug repurposing in Claudin-low breast cancer subtype

Υπολογιστική φαρμακευτική επαναστόχευση στο Claudin-low υποείδους του μαστικού καρκίνου

Ioannis S. Kontos

Examination Committee:
Thireou Trias, Assistant Professor AUA (supervisor)
Douni Eleni, Professor AUA
Triantafyllopoulos Konstantinos, Assistant Professor AUA

Computational drug repurposing in Claudin-low breast cancer subtype

Msc Systems Biology
Department of Biotechnology

ABSTRACT

Claudin-low (CL) subtype of breast cancer is characterized by low gene expression of tight junction proteins claudin 3, 4 and 7 and E-cadherin, and by high expression of genes participating in the epithelial-mesenchymal transition (EMT). Despite its clinical significance, there is limited understanding regarding the cellular origin and the specific oncogenic drivers that contribute to its development and progression. Within this context, the MSc dissertation aimed at providing insight into the CL mechanism and at computationally identifying candidate repurposed FDA-approved drugs. To this end, we used network analysis and two in silico drug repurposing techniques, namely docking and gene expression profile reversing. The network analysis of the upregulated CL genes signature showed that, based on nodes centrality, the most influential genes were the *CD44, JUN* and *TGFBR2*. These genes were found to be associated through a positive regulation loop, primarily activating the ERK pathway. Next, we performed docking of FDA-approved compounds to ANPEP, a protein found upregulated in CL and proposed as a therapeutic target. We also compiled a list of molecules that reverse the genetic signature of CL. Two shared drugs between those two lists, Olanzapine and Pantoprazole, were shown to reduce the migratory ability of cancer, by inhibiting both ANPEP and ERK pathway. Molecular dynamics simulations of the predicted complexes were performed to investigate if the compounds acquired stable conformations in the docked poses within ANPEP. Additionally, the analysis of the gene ontology terms of the proteins targeted by the compound lists showed that the term GABA alpha-receptor (GABAAR) was enriched among all gene lists, indicating that most compounds indirectly affect it. The particular receptor is upregulated in breast cancer and is found to utilize the ERK 1/2 signaling pathway to mediate pro-migratory effects. The research suggests the significance of the ERK1/2 pathway, as the main mediator of the epithelial-mesenchymal transition (EMT), in the formation/progression of CL. ERK is involved in a variety of cellular processes making it harder to target without causing significant side effects. GABAAR is proposed as a therapeutic target, as hyperactivation of the receptor is shown to induce apoptosis. Further in silico and experimental studies are necessary to validate the candidate-repurposed drugs.

Scientific area: Bioinformatics

Keywords: Drug repurposing, breast cancer, claudin-low, molecular dynamics, molecular docking, connectivity map

Υπολογιστική φαρμακευτική επαναστόχευση στο Claudin-low υποείδους του μαστικού καρκίνου

ΠΜΣ Βιολογία Συστημάτων
Τμήμα Βιοτεχνολογίας

ΠΕΡΙΛΗΨΗ

Το υποείδος του καρκίνου του μαστού Claudin-low (CL) χαρακτηρίζεται από μειωμένη γονιδιακή έκφραση των πρωτεϊνών claudin 3, 4 και 7, και e-cadherin και από την υπερέκφραση γονιδίων που συμμετέχουν στην επιθηλιακή-μεσεγχυματική μετάβαση (EMM). Παρα την κλινική του σημαντικότητα, υπάρχει περιορισμένη κατανόηση σχετικά με την κυτταρική προέλευση του, και τους συγκεκριμένους ογκογενείς παράγοντες που συμβάλλουν στην ανάπτυξη και εξέλιξή του. Στο πλαίσιο αυτό, η μεταπτυχιακή διατριβή στοχεύει στο να συμβάλλει στην κατανόηση του μηχανισμού του CL, αλλά και στην υπολογιστική ταυτοποίηση υποψήφιων FDA-εγκεκριμένων φαρμάκων για επαναστόχευση σε αυτόν. Για αυτόν τον σκοπό, πραγματοποιήθηκε ανάλυση δικτύου και δύο υπολογιστικές (in silico) τεχνικές φαρμακευτικής επαναστόχευσης, την πρωτεϊνική σύνδεση (protein docking) και την αντιστροφή της γονιδιακής έκφρασης του CL. Η ανάλυση δικτύου των υπερεκφραζόμενων γονιδίων του CL, βασιζόμενη στην ανάλυση της κεντρικότητας των κόμβων, έδειξε ότι τα γονίδια CD44, JUN και TGFBR2, εμφανίζουν την μεγαλύτερη επιρροή στο δίκτυο. Αυτά τα γονίδια φαίνεται ότι μετέχουν σε μια θετικά ρυθμιζόμενη λούπα, υποκινούμενη από την ενεργοποίηση του μονοπατιού EPK. Στη συνέχεια πραγματοποιήθηκε η πρωτεϊνική σύνδεση των FDA-εγκεκριμένων μορίων στην πρωτεΐνη του ANPEP, η οποία βρέθηκε να υπερεκφράζεται στον CL και αποτελεί δυνητικό θεραπευτικό στόχο. Επίσης, συντάξαμε δύο λίστες μορίων ικανά να αντιστρέψουν την γενετική υπογραφή του CL. Τα κοινά φάρμακα που βρέθηκαν από τις δύο υπολογιστικές τεχνικές, Olanzapine και Pantoprazole, έδειξαν να μειώνουν την μεταναστευτική ικανότητα του καρκίνου, παρεμποδίζοντας την ANPEP αλλά και το μονοπάτι ERK. Ακολούθως, εφαρμόστηκαν μοριακές δυναμικές προσομοιώσεις των προβλεπόμενων συμπλόκων με σκοπό να διερευνηθεί αν τα μόρια αποκτούν σταθερές διαμορφώσεις κατά την σύνδεση τους με την ANPEP. Τέλος, η ανάλυση των γονιδιακών οντολογικών όρων των γονιδίων που επηρεάζονται από τα μόρια των λιστών που συντάχθηκαν, έδειξε ως κοινό τους όρο τον υποδοχέα GABA alpha receptor (GABAAR), υποδεικνύοντας ότι επηρεάζεται έμμεσα από τα περισσότερα μόρια. Η υπομονάδα πι του συγκεκριμένου υποδοχέα, παρατηρείται να υπερεκφράζεται στον καρκίνο του μαστού, και να ενεργοποιεί το μονοπάτι ERK για την απόδοση των μεταναστευτικών ιδιοτήτων. Η έρευνα υποδεικνύει τη σημαντικότητα του μονοπατιού ERK, ως τον κύριο διεκπεραιωτή της επιθηλιακής-μεσεγχηματικής μετάβασης, στον σχηματισμό και στην ανάπτυξη του CL. Το ERK συμμετέχει σε πληθώρα κυτταρικών διεργασιών, καθιστώντας δύσκολη τη στόχευση / καταστολή χωρίς παρενέργειες. Το GABAAR προτείνεται ως θεραπευτικός στόχος, μιας που η υπομονάδα πι μπορεί να επηρεάσει έμμεσα το μονοπάτι EPK. Τέλος τα μόρια Olanzapine και Pantoprazole προτείνονται για περαιτέρω ανάλυση μέσω πειραματικών διεργασιών για την πιθανότητα επαναστόχευση τους στον CL.

Επιστημονική περιοχή: Βιοπληροφορική

Λέξεις κλειδιά: Φαρμακευτική επαναστόχευση, καρκίνος μαστού, μοριακή πρόσδεση

ACKNOWLEDGEMENTS

I would like to thank my supervisor, Dr Thireou Trias, for guiding me through the concepts and perspectives of bioinformatics. Her feedback and support helped me improve my skills to effectively analyse and communicate this project. I would like to give special thanks to my Erasmus+ traineeship supervisor Valverde J. Ramon, for providing me extra support and the resources needed to conduct important computational analyses.Finally, I would like to thank my committee members, Dr Douni and Dr Triantafyllopoulos, for serving on my thesis committee and providing helpful feedback and suggestions.

With my permission, this work has been checked by the advisory & examination committee through the plagiarism identification software available from AUA, verifying its validity and originality.

CONTENTS

1. INTRODUCTION

1.1 Breast cancer Overview

Breast cancer (BC) is a highly heterogeneous group of diseases with variable biological and clinical behaviour. The different BC types can be classified based on different factors, including the presence or absence of certain genetic mutations, the expression of different proteins, and the tumour's growth pattern and stage. These factors not only influence the tumour's behaviour and response to treatment, but the overall prognosis as well. Gene-expression profiling analyses provided insight into the diversity of the molecular subtypes, known as intrinsic subtypes. According to the PAM50 classification these subtypes are luminal A, luminal B, HER2-enriched and basal-like (Prat et al., 2010). An additional intrinsic subtype of BC, known as claudin-low (CL), has recently been identified in human and mouse tumours, in BC cell lines. CL shows several common features with basal-like tumours, reflecting the diversity of tumours with a low luminal differentiation status (Prat et al., 2010).

1.2 Breast Cancer Subtypes and Claudin-low

Luminal A is the most common subtype, accounting for about 40% of all breast cancers. It is characterised by the presence of oestrogen and/or progesterone receptors (ER/PR) on the tumour cells, typically showing low levels of HER2 expression and a low proliferation rate. Luminal B, on the other hand, shows a more aggressive profile, with higher levels of HER2 expression and a higher proliferation rate, without necessarily being ER/PR positive. HER2-enriched tumours are characterised by overexpression of the HER2 protein on the surface of tumour cells. Although HER2-enriched cells are similar to luminal B, they have a higher risk of recurrence, and are less likely to express oestrogen and/or progesterone receptors. The determination of the subtype in BC is important in guiding treatment decisions and predicting the prognosis of the disease.

Triple-negative breast cancers (TNBCs) are an aggressive subgroup of breast malignancies defined as tumours lacking expression of the oestrogen receptor (ER), progesterone receptor (PR), and HER2 (Lenhmann et al., 2011). Basal-like and claudin-low tumours form the majority of TNBCs, sharing common features, but distinct molecular and genetic characteristics. Basal-like is characterised by the expression of genes that are typically found in basal cells, which line the mammary ducts. It tends to have a higher expression of genes involved in cell cycle regulation and DNA repair, whereas claudin-low has a higher expression of genes involved in cell migration and invasion.

CL tumours reflect characteristics of their intrinsic subtype, as they are distinguished by low genomic instability and mutational burden, consisting of a predominant population of triple-negative mammary tumour cells (Fougner et al., 2020). These cells exhibit

characteristics reminiscent of stem cells and display mesenchymal features (Radler et al., 2021).

The genetic profile of CL is characterised by low expression of the calcium-dependent glycoprotein E-cadherin, and tight junction proteins claudin 3, 4 and 7, responsible for cell-cell adhesion (Lenhmann et al., 2011). And by the high expression of genes participating in the epithelial-mesenchymal transition (EMT), during which epithelial cells lose their polarity and cell-cell adhesion. Cytoskeletal reorganisation and loss of E-cadherin are important steps in this transition; thus, CL tumours gain migratory and invasive properties (Bhatt et al., 2021).

Despite its clinical significance, there is limited understanding regarding the cellular origin and specific oncogenic drivers that contribute to the development and progression of CL (Radler et al., 2021). This result can be attributed to the unique challenges it poses, due to its distinct molecular profile and limited knowledge about its underlying mechanisms. Thus, there is a growing demand for further research to unravel the cellular origins of claudin-low breast cancer (CLBC) and to identify the specific oncogenic drivers responsible for its aggressive profile (Radler et al., 2021). Such investigations hold the potential to uncover novel therapeutic targets and treatment strategies for this challenging subtype of BC (Radler et al., 2021). Overall, identifying the specific subtype is crucial for determining the best course of treatment for each patient, as different subtypes respond differently to various therapies.

1.3 Drug repurposing

Drug repurposing, also known as drug repositioning or therapeutic switching, is the process of identifying new therapeutic uses for existing drugs that have already been approved for human use. According to certain reports, approximately 30-40% of novel drugs and biologics that received approval from the US Food and Drug Administration (FDA) between 2007 and 2009 could be categorised as repurposed or repositioned products (Graul et al., 2009). Similarly, a research study discovered that 35% of transformative drugs endorsed by the FDA from 1984 to 2009, which were characterised as both innovative and having groundbreaking effects on patient care were actually repurposed products (Krishnamurthy et al., 2022). Many experts argue that repurposing drugs may offer advantages in terms of speed, cost-efficiency, reduced risk, and higher success rates compared to traditional drug development methods (Krishnamurthy et al., 2022). This is primarily because researchers can bypass the earlier phases of development that focus on establishing drug safety, as these stages have already been completed and the safety and pharmacokinetic properties of the drug have been already established. Therefore, repurposing enables the expansion of treatment options for patients by identifying new uses for existing drugs (Krishnamurthy et al., 2022).

It has been suggested by some reviews that around 30% of repurposing endeavours achieve success, resulting in FDA-approved marketable products. In contrast, the success rate for new drug applications in general, hovers around 10% (Hauser et al., 2017). However, there is contradictory evidence suggesting that repurposed agents do not necessarily outperform new agents, with their effectiveness, rather than safety, often being their limiting factor (Krishnamurthy et al., 2022).

Reports indicate that the process of de novo drug discovery and development can span a lengthy 10-to-17-year period. Conversely, repurposed drugs typically receive approval much sooner, within a range of 3 to 12 years, and at approximately half the cost (Novack, 2021). During the Covid-19 pandemic, there has been a renewed focus on drug repurposing, notably after the FDA granted emergency use authorization (EUA) for several repurposed drugs to treat Covid-19 (Novack, 2021). For instance, within six months of the pandemic's onset, the FDA issued a EUA for remdesivir, marketed as Veklury. Prior to its authorization as a Covid-19 treatment, remdesivir hadn't received FDA authorization for its original design as an antiviral for RNA-based viruses (Krishnamurthy et al., 2022). Despite the enthusiasm surrounding drug repurposing, there has been a lack of systematic literature reviews examining why pharmaceutical companies often reprioritize or abandon promising drug candidates that have not received FDA approval for any indication. In addition, there has been a dearth of research exploring the factors that either hinder or facilitate the process of bringing these promising compounds off the shelf and back into development, commonly referred to as drug repurposing (Krishnamurthy et al., 2022).

Several computational approaches coupled with open-access databases have been described as instrumental in predicting drug-disease responses and validating targets and pathways, thus advancing repurposing endeavours (Pulley et al., 2018). Among these newer methods, signature-based approaches have been commonly employed for drug repurposing. Such approaches identify alternative indications for existing drugs by investigating published GWAS data from institutes such the US National Human Genome Institute (Krishnamurthy et al., 2022). However, key limiting factors are the expertise and time required to develop such assays and the integration of databases that identify known drugs among confirmed activities (Swamidass, 2011).

In-silico screening of compound libraries is important in both significantly reducing wet-laboratory work and lowering the cost of experimental determination of drug-target interactions (Wang & Weng, 2013).

Additionally, an effective and economical strategy for repurposing drugs is the mining of open-access phenotypic screens of small molecules (Swamidass, 2011). Bioinformatics-based approaches are able to identify closely related targets and new repurposing opportunities, utilizing tools for domain similarity prediction and sequence alignment to discover novel protein–protein similarities. Additionally, chemoinformatics-based

approaches utilize computational algorithms that rank and prioritise compounds for experimental testing, based on the molecular representations of candidate compounds. Such example is the molecular docking method used to screen several compounds against a target protein, with known 3D structure (Wang & Zeng, 2013).

Network modelling and systems-biology approaches have also been discussed as valuable techniques. Network modelling involves the reconstruction of a biological network and the simulation of its interactions to reveal potential drug targets (Shahreza et al., 2018). A systems-biology approach involves the utilisation of omics data, signalling pathways, metabolic pathways, and protein interactions to propose a new pathway for a given disease (Katare & Banerjee, 2016). Limitations of such approaches, in their predictions of how drugs and targets interact, are tackled by the use of machine learning which is able to accurately predict drug-target interactions, inferring modes of action, and establishing novel drug-target relationships (Wang & Zeng, 2013). Finally, the utilisation of Artificial Intelligence (AI)-driven technology has been introduced as a means to integrate diverse types of data and search for connections. Such example is the project prodigy, an AI solution developed by Biovista, with the capability to construct entirely new clinical scenarios, resulting in repurposing successes in the fields of multiple sclerosis and epilepsy (Challener, 2018). Their AI system has been applied in collaboration with major pharmaceutical companies, patient advocacy groups, and the FDA (Challener, 2018).

1.4 Examples of repurposed drugs

Examples of drugs that have been successfully repurposed or repositioned in various medical contexts are frequently discussed in the literature, including repurposing for rare and neglected diseases, including Alzheimer's disease, AIDS, and central nervous system disorders. The literature highlights several instances of drugs that have been effectively repositioned. These include thalidomide, Viagra® (sildenafil), Saracatinib, AZT, Aducanumab, Sunitinib, Tamoxifen, Raloxifene, and Trastuzumab (Krishnamurthy et al., 2022).

In the field of drug development, there is a concept known as "drug promiscuity," which refers to the idea that a single drug can have an impact on multiple pathways, potentially leading to new applications for drug candidates. Thalidomide is frequently cited as a prime example of this phenomenon. Originally produced by the German company Chemie Grunenthal in the 1950s, thalidomide faced setbacks and was withdrawn from several markets due to its teratogenic effects (Chesbrough & Chen, 2013). Notably, it had not received approval from the US FDA at that time. However, subsequent research revealed that thalidomide could inhibit tumour necrosis factor-alpha signalling. As a result, it found new purpose in the treatment of erythema nodosum leprosum, a serious complication of leprosy, and later in multiple myeloma. Although it was approved by the FDA for acute

erythema nodosum leprosum in 1998, its usage remained restricted due to stringent guidelines (Chesbrough & Chen, 2013). Another well-known example, Viagra®, initially demonstrated a lack of efficacy during clinical trials for its intended use. However, its unusual side effects and unsuitable pharmacokinetic properties for angina treatment led to its eventual repurposing for the treatment of erectile dysfunction (Chesbrough & Chen, 2013).

Saracatinib, initially designed for various oncology applications, was deprioritized following limited efficacy observed in phase II studies. The inspiration for repurposing this drug emerged from the discovery of memory impairments in Alzheimer's disease mouse models and data linking Fyn tyrosine kinase phosphorylation to Aβ and tau-related synaptic dysfunction (Frail et al., 2015). Saracatinib is currently under investigation for alternative uses, including bone pain and lymphangioleiomyomatosis (Frail et al., 2015).

The case of Azidothymidine (AZT) illustrates the potential of comprehensive understanding of disease and drug mechanisms in discovering new applications. Originally explored as a chemotherapy drug in the 1960s, AZT was discarded due to its ineffectiveness. However, its antiretroviral properties were recognized during the early stages of the HIV epidemic (Cha et al., 2018). Collaborative efforts between National Institutes of Health (NIH) and industry experts repurposed the drug, making it the first HIV treatment (Cha et al., 2018).

Initially abandoned due to unfavourable results from an independent monitoring committee's futility analysis, Aducanumab was revitalised through a re-examination of data from two unsuccessful clinical trials. Notably, patients receiving the highest dose exhibited a statistically significant reduction in cognitive decline and improved basic daily living activities. Biogen contested the accuracy of the initial analysis, receiving FDA approval to reintroduce the nearly abandoned drug (Cortez & Langreth, 2019).

Sunitinib serves as an example of successful on-target repurposing. Despite failures in clinical trials for various cancers, including colorectal, breast, prostate, and non-small cell lung cancer, it found success in treating gastrointestinal stromal tumours and renal cancers after repurposing efforts. In 2010, it obtained approval for pancreatic neuroendocrine tumour treatment, emphasising the significance of a targeted approach in repurposing (Naylor & Schonfeld, 2014).

Tamoxifen, initially developed as a contraceptive and orphan drug, later displayed efficacy in inducing ovulation in sub-fertile women and treating postmenopausal women with metastatic breast cancer in translational laboratory studies (Jordan, 2003). As a nonsteroidal antiestrogen, tamoxifen was repurposed, gaining approval for treating metastatic breast cancer and reducing breast cancer risk (Jordan, 2003). It currently stands as the standard therapy for long-term adjuvant treatment of oestrogen receptor-positive breast cancer.

A series of translational studies conducted in the 1970s and 80s focused on the uterus, breast, and bone, creating a foundation for further research and trials. This effort led to the reintroduction of, the initially failed, keoxifene into raloxifene—the first clinically available selective oestrogen receptor modulator for preventing breast cancer and osteoporosis.

Trastuzumab, which is a monoclonal antibody initially approved for the treatment of HER2-positive breast cancer, has now gained approval for the treatment of HER2-positive advanced gastric and gastroesophageal junction cancer as well (To & Cho, 2022). This expansion of trastuzumab's indications reflect a process known as "soft repurposing," where existing oncological drugs are repurposed for new applications in different cancer types (To & Cho, 2022). Additionally, Pantziarka et al. (2018) categorised the repurposing of non-oncology drugs for cancer treatment as "hard repurposing". This term refers to the utilisation of drugs originally developed for non-cancer-related purposes in the treatment of cancer (Pantziarka et al., 2018). This classification highlights the innovative approaches being explored to identify potential therapeutic options for various cancer types.

2. RESEARCH PURPOSE

The purpose of the research is to investigate the CL mechanism and to propose candidate FDA-approved drugs for repurposing, by employing several computational methods. In particular, network analysis and functional annotation clustering indicated the significance of the ERK1/2 pathway as the main mediator of the epithelial-mesenchymal transition (EMT), in the formation/progression of CL. The in silico drug repurposing techniques docking and gene expression profile reversing resulted in two lists of candidate compounds. The lists intersection highlighted two drugs, which were further studied using molecular simulation techniques.

3. METHODS

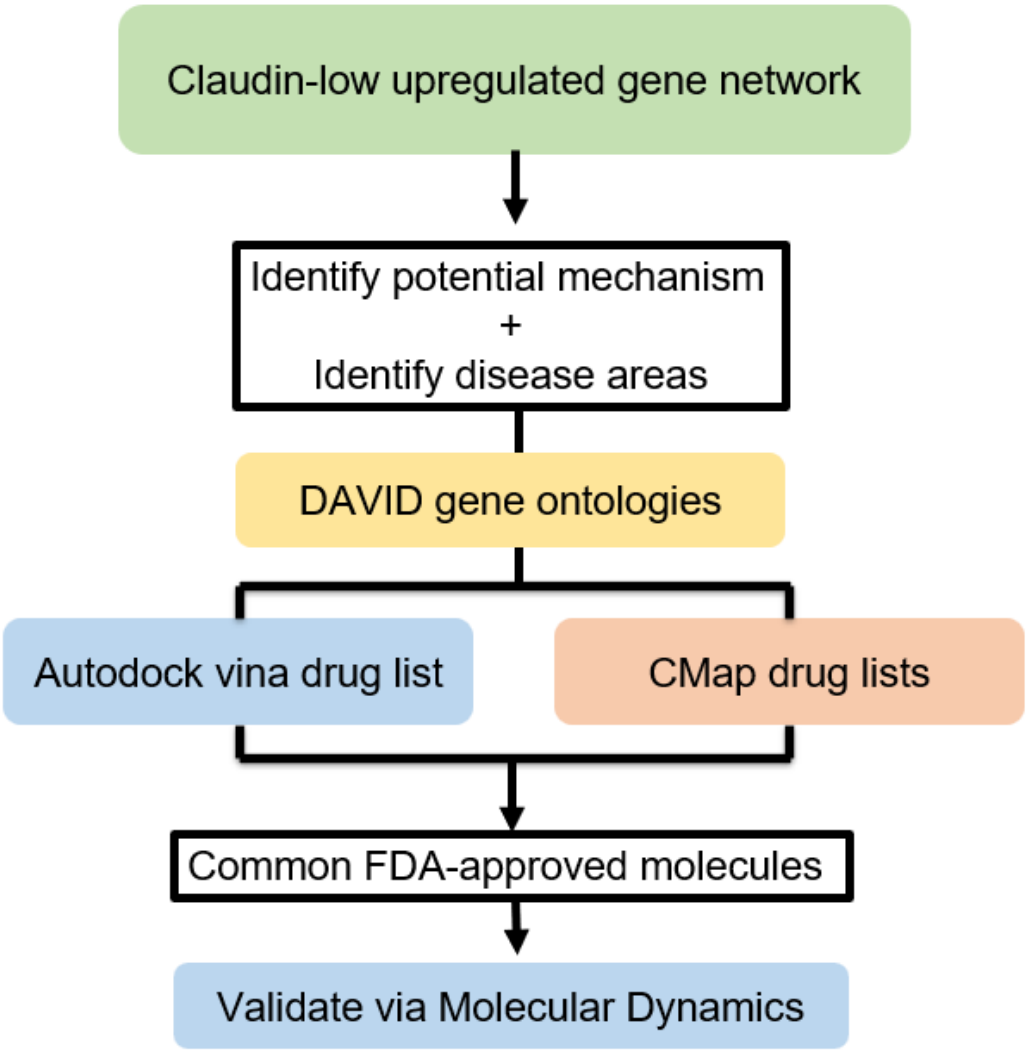

Figure 1. Workflow pipeline of the methods used in this study.

3.1 Genetic signature network analysis using Cytoscape

The upregulated genes of the claudin low genetic signature, identified by Papamichail (2023) were imported in string database (Szklarczyk et al., 2015). The resulting network was loaded in Cytoscape and analyzed using the Network Analyzer plugin. The plugin is suitable for studying the properties of biological networks such as gene regulatory networks, protein-protein interaction networks, and metabolic networks (Shannon et al., 2003). The analysis of the network poses the first step of the pipeline developed for this research **(fig1.)**.

In the context of biological gene networks, betweenness centrality and closeness centrality are commonly used to identify key genes involved in the regulation of gene expression and signalling. Betweenness centrality is calculated based on the number of shortest paths that pass-through a given node, which reflects the importance of that node as a bridge between different regions of the network. Genes with high betweenness centrality are thus considered to be critical in maintaining the overall connectivity and flow of information in the network. On the other hand, closeness centrality is calculated based on the average distance from a given node to all other nodes in the network, which reflects the efficiency of that node in transmitting signals to other parts of the network. Genes with high closeness centrality are thus considered to be central in the network and may play an important role in coordinating biological processes. Both measures have been shown to be useful in identifying key genes and pathways in biological gene networks, which can provide insights into the underlying molecular mechanisms of biological processes and potential therapeutic targets for diseases involving disruptions in gene regulation or signalling.

3.2 Genetic signature analysis using Connectivity map

In the Connectivity Map (CMap), a detailed collection of cellular signatures has been compiled, representing organized alterations caused by both genetic (reflecting protein function) and pharmacological (reflecting small-molecule function) factors. Similar signatures may indicate potential connections, such as between proteins in the same pathway, a small-molecule and its target protein, or between structurally different small-molecules with similar functions (https://clue.io). The 29 upregulated genes of the CL genetic list were imported into the CLUE (CMap and LINCS Unified Environment) QUERY tool. The genetic library BING utilised by the CMap 1.0 version included 28 of the input upregulated genes. The tool generated a list with molecules able to enhance or reverse the uploaded genetic signature. The tool scored each molecule with a tau value between -100 and +100, with the lowest score indicating the highest correlation of genetic signature reversal. For example, tau= -90 indicated that only the 10% of the molecules from the Touchstone dataset, tested on the same cell line, showed stronger reversal of the genetic signature than the molecule of interest (scored -90). Bioactive compounds of Tau > 90 and <-90 show statistical significance, for enhancing or reversing the genetic signature, respectively. The output results could be reviewed by showcasing 150 bioactive compounds, derived from 9 different cell lines, with a maximum tau score of -90. In general, it was considered that tau scores of +90 or higher, and of -90 or lower, were to be considered as hypotheses for further study (https://clue.io). The compounds were further filtered to be only FDA approved compounds, resulting in a list of 38 total compounds (**Supplementary Table 2).** The genes that were targeted by the extracted compounds were used to isolate their gene ontology terms. Finally, the same procedure was followed but only using the compounds generated from the MCF7 cell line. The

resulting list consisted of 66 FDA approved molecules (**Supplementary table 3**). The FDA approved molecules derived from connectivity map were analysed using the Broad id identifier to categorise them into different disease areas.

3.3 Gene ontologies of the targeted genes

The gene ontologies of the genes that are targeted by the compounds of the lists CM and MCF7 were extracted, clustered using the DAVID program, and analysed to identify shared clusters. The enrichment score reflected the degree of over-representation of a specific functional category in a cluster of related categories (Huang et al., 2009). The clustering analysis grouped functionally related terms based on their similarity and assigned an enrichment score to each cluster. The enrichment score for a functional annotation cluster was calculated as the geometric mean of the enrichment scores for the individual annotation terms within the cluster (Huang et al., 2009). A higher enrichment score for a cluster indicated a stronger degree of enrichment for the corresponding biological process, molecular function, or cellular component, and suggested that the cluster was biologically relevant to the input gene list. Similar to the individual annotation term analysis, a score of 1.3 or higher was used as a significance threshold for the functional annotation clustering analysis (Huang et al., 2009).

3.4 Docking analysis of ANPEP USING Autodock Vina

A protein that participates in the EMT, the mammalian aminopeptidase N (ANPEP) shows great potential as a therapeutic target for the treatment of diseases related to many physiological processes like blood pressure regulation, tumour angiogenesis and metastasis, immune cell chemotaxis, sperm motility, cell-cell adhesion, and coronavirus entry (Hen et al., 2012). This protein was selected after extensive literature research as a potential therapeutic target for performing molecular docking.

Docking results were generated for the ANPEP with all FDA approved drug molecules, including Ezetimibe, ANPEP`s known inhibitory compound, using Autodock vina. AutoDock Vina is a software program used to predict the binding affinity of a small molecule ligand to a protein receptor. Before running Vina, it's essential to prepare the protein receptor and the small molecule ligand. This involves removing any water molecules or other unwanted structures from the protein structure and optimising the ligand structure. Once the protein and ligand structures are prepared, a grid is generated around the protein receptor to define the search space for the ligand. This grid is used to calculate the interaction energy between the protein and the ligand. Vina performs a docking simulation by systematically exploring the search space defined by the grid and predicting the binding affinity of the ligand to the protein. The software uses a genetic algorithm to perform this search and optimise the binding energy score. Once the docking

simulation is complete, AutoDock Vina generates a list of predicted binding poses (conformations) and associated binding energies for the ligand (Eberhardt et al., 2021).

Vina reports the binding energy of each predicted binding pose of the ligand. These binding energies are expressed in units of kcal/mol and represent the free energy change associated with the formation of the protein-ligand complex from the separated components (Eberhardt et al., 2021). A more negative binding energy (i.e., a larger absolute value) indicates a stronger binding interaction between the protein and the ligand, and therefore a higher predicted binding affinity. Molecules with binding affinity lower than the known molecule were filtered out (**Supplementary Table 1**)**.** The FDA approved molecules derived from VINA were analysed using the Broad id identifier to categorise them into different disease areas.

The gene ontologies extracted from the Vina, CM, MCF7 drug lists, and upregulated genes of the claudin-low signature, were clustered using the functional annotation clustering option of DAVID program. Moreover, the three drug lists generated were compared, to find shared compounds (**fig1.**). The resulting compounds were used to find their gene targets and create a network with the upregulated genes of the genetic signature, in order to observe possible interactions, using the Cytoscape software.

3.5 Molecular dynamics

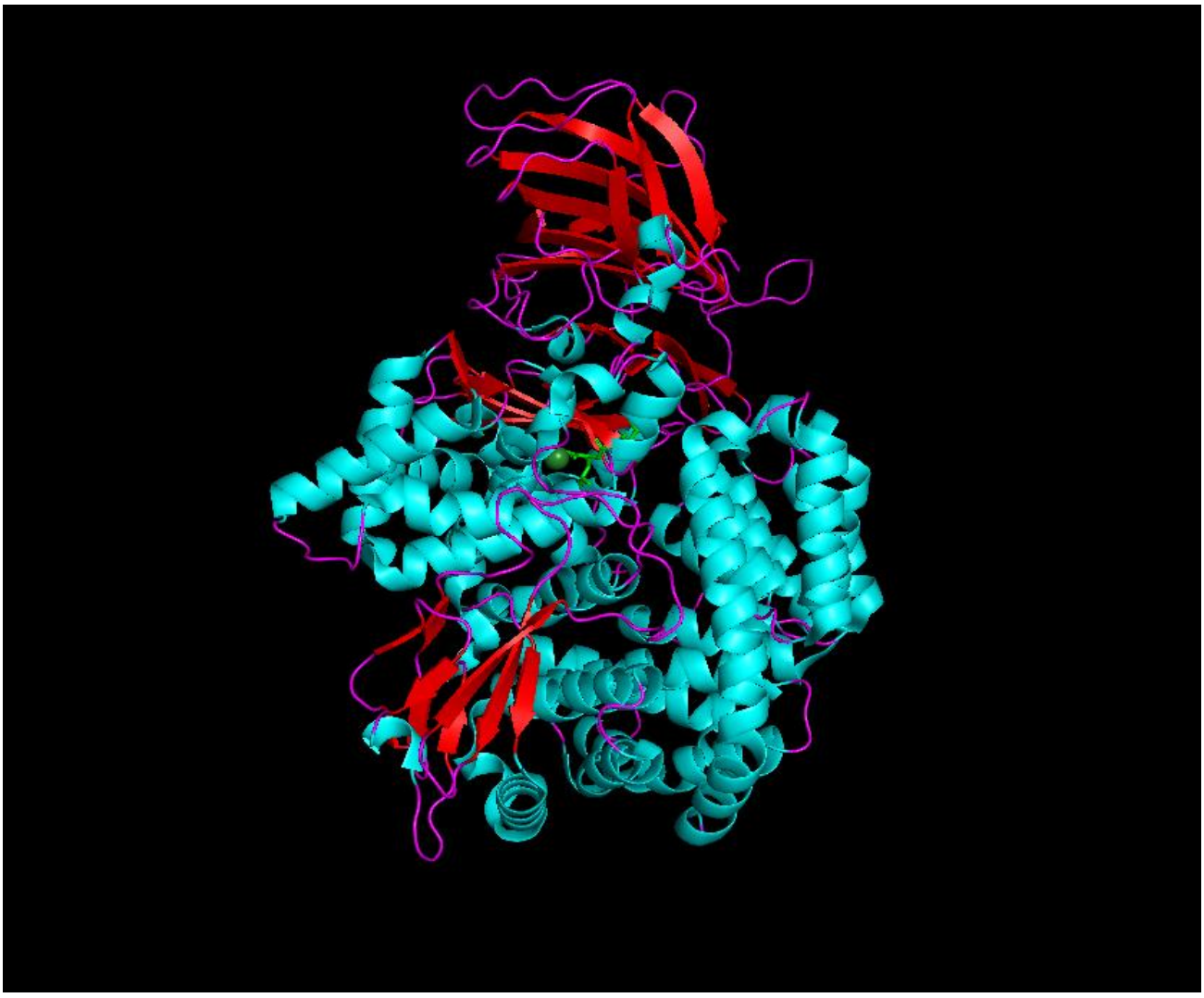

Figure 2. Aminopeptidase-N (ANPEP) complex with Bestatin (protein data bank id: 4FYR). The alpha helices of the ANPEP protein are shown in cyan, the beta sheets in red and the loops in magenta, while the ZN is shown in dark green and the Bestatin molecule in green.

Based on the docking and CM results and literature research of the four shared molecules, we selected only Pantoprazole and Olanzapine choosing four and three different conformations, respectively (**fig3.**). For the reference protein structure, we used the experimentally characterised ANPEP-Bestatin complex (pdb: 4FYR), as Bestatin is a known natural inhibitor of ANPEP (Chen et al., 2012) (**fig2.**). The pdb files of all the conformations generated from Autodock Vina were used to make pdb files of the protein-ligand complexes, using the Chimera software.

The complexes were processed using PoseView to generate a graphical representation of their protein-ligand interaction profile. PoseView automatically generates 2D diagrams of molecular complexes, focusing on the interaction network between the complex partners (Stierand et al., 2010). Computing collision-free layouts by representing the interacting molecules on the atomic level following the IUPAC recommendations for the depiction of structured diagrams (Stierand et al., 2010).

The files of each complex were used as input in the charmm-gui solution builder generator. For the next steps, the Antechamber option was selected to generate top and par files, automatically generating the customised FF parameters for the molecule, uploaded in SDF format. In addition, two pairs of disulfide bonds were defined, which are known to appear in ANPEP. The TIP3P water box size was set to "rectangular" and defined to fit the protein size with an edge distance of 12Å. Finally, ions were added using the Monte-Carlo ion placing method, and the generated input files for GROMACS software were downloaded. MD simulation was carried out with the GROMACS 4.6.5 suite of programs using the CHARMM36m force field. Periodic boundary conditions were employed using the particle mesh Ewald (PME) method for long-range electrostatics interactions. The Na+ counterions were added to satisfy the electroneutrality condition.

Initially, energy minimization and equilibration of all systems was executed through following three steps: (i) Energy minimization of all systems containing ions, solvent, receptor, and ligand was executed using the steepest descent minimization algorithm with 5000 steps to achieve stable systems with maximum force < 1000 kJ mol nm. (ii) Position restrains were applied to receptor and ligand of each system for 100 ns throughout heating (300 K) utilising NVT (No. of atoms, Volume, Temperature) ensemble with leap-frog integrator, a time step of 2 fs and LINCS holonomic constraints. (iii) NPT (No. of atoms, Pressure, Temperature) ensemble was applied at a constant pressure (1 bar) and temperature (300 K) for 100 ps using a time step of 2 fs for NPT equilibration phase. After the energy minimization and equilibration of all systems, MD production run was executed without any restrain for 50 ns with a time step of 2 fs, and the coordinates of the structure were saved every 10 ps. After the completion of 50 ns MD simulation, the trajectories were used for various dynamic analysis such as root mean square deviation (RMSD), root mean square fluctuation (RMSF), and radius of gyration (Rg).

4. RESULTS

4.1 Genetic signature network analysis

Table 1. Network analyzer table from Cytoscape, showcasing the top nodes based on the centrality of each node.

display name	BetweennessCentrality	ClosenessCentrality	Degree
SNAI2	0.02	0.5	6
VIM	0.03	0.51	8
ANXA1	0.03	0.48	4
ZEB2	0	0.45	5
JUN	0.29	0.61	9
PBK	0	0.33	1
TGFBR2	0.17	0.56	9
CD274	0.07	0.51	6
CSF1R	0.1	0.49	5
CCNB1	0.18	0.49	5
CALR	0.18	0.47	4
SNCA	0	0.39	2
PTGS2	0.04	0.5	5
CD44	0.21	0.61	13
ADAM12	0	0.37	1
PTTG2	0	0.33	1
TWIST1	0	0.46	6
SERPINH1	0.09	0.33	2
THY1	0.02	0.46	6
CRTAP	0	0.25	1
LAPTM5	0	0.33	1
ZEB1	0.03	0.51	7
EPAS1	0	0.39	1

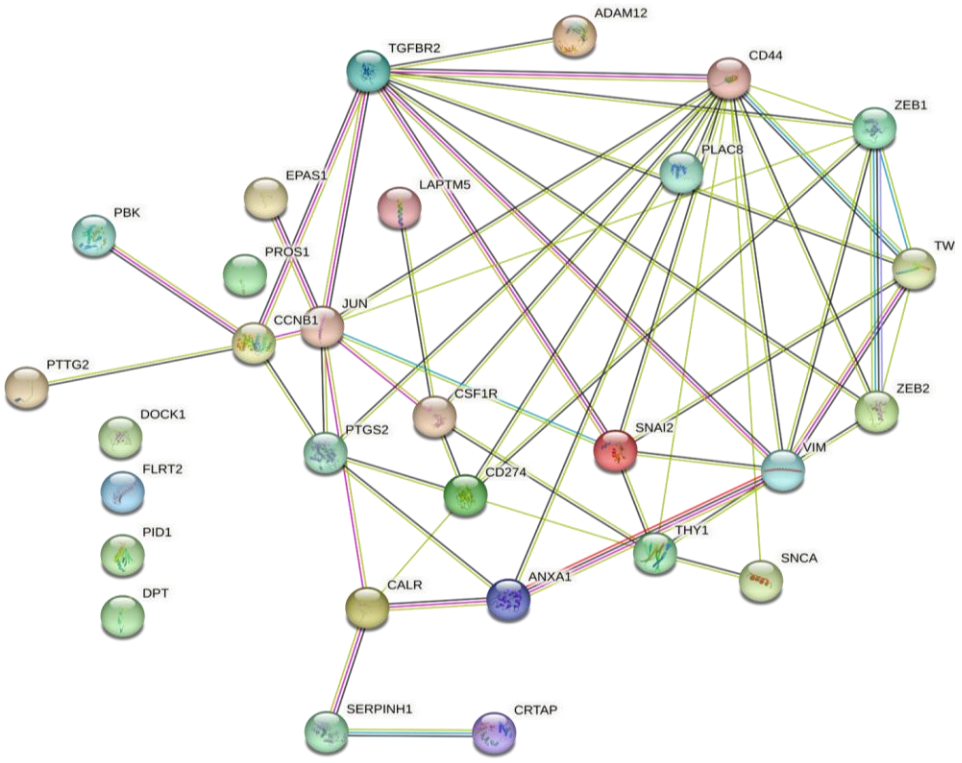

Figure 3. Network of the claudin-low genetic signature generated by the string database.

In order to identify relevant and specific therapeutic targets to CL, the upregulated genetic signature of CL was utilized as determined by Papamichail (2023). The potentially important upregulated genes identified in CL are *VIM, SNAI2, TWIST1, ZEB1, ZEB2, THY1, PBK, CCNB1, SNCA, PTTG2, CRTAP, TGFBR2, PROS1, FLRT2, PID1, ANXA1, LAPTM5, PLAC8, ADAM12, DOCK1, PTGS2, CD274, DPT, EPAS1, CSF1R, SERPINH1, CALR, CD44, JUN*. The network of upregulated genes was created in Cytoscape and analyzed to identify the most influential nodes. Non connected nodes, including *DOCK1, FLRT2, PID1, DPT, and PROS1*, were opted out of the analysis (**fig3B.**). To understand the relationships between these genes, the network analysis used degree centrality, betweenness centrality, and closeness centrality metrics (**fig3A.**). Degree centrality is a measure of the number of connections (edges) that a node has in a network. In the context of this analysis, the top 3 nodes with the highest degree centrality are *CD44, JUN*, and *TGFBR2*. *CD44* has the highest degree centrality with a value of 13, indicating that it is highly connected in the network. *JUN* and *TGFBR2* both have a degree centrality of 9, indicating that they are also highly connected. These results suggest that *CD44, JUN, TGFBR2* are potentially important nodes in the network and may play a critical role in the disease process. *CD44* stands out with the highest degree centrality value, indicating that it may be a key therapeutic target.

Betweenness centrality is a measure of how important a node is in facilitating the flow of information between other nodes in a network. In this analysis, the top three nodes based on betweenness centrality are *JUN, CD44, and with the same scores, CCNB1* and *CALR*. *JUN* has the highest betweenness centrality value (0.289), indicating that it is a key mediator of communication between other nodes in the network, as it is located on many of the shortest paths connecting pairs of other genes in the network. JUN is a transcription factor that plays a role in many cellular processes, including cell proliferation, differentiation, and apoptosis. *CD44, CCNB1* and *CALR* have betweenness values of 0.208, 0.18 and 0.18, respectively, indicating that they also play a role in connecting different parts of the network. This cluster may represent key genes that act as bridges between different regions of the network and are essential for information flow.

The third ranking identified by the closeness centrality measure consists of *CD44, JUN,* and *TGFBR2*, with *CD44* and *JUN* having the highest closeness values of 0.611. This suggests that *CD44* and *JUN* are located close to most other genes in the network and may play a central role in information transfer. *TGFBR2* also has a high closeness value of 0.564, indicating it is also centrally located in the network. This cluster may represent key genes that are essential for efficient communication between different parts of the network. These findings provide insight into the potential functional relationships and roles of these genes within the network and could be used to generate new hypotheses or predictions for further investigation.

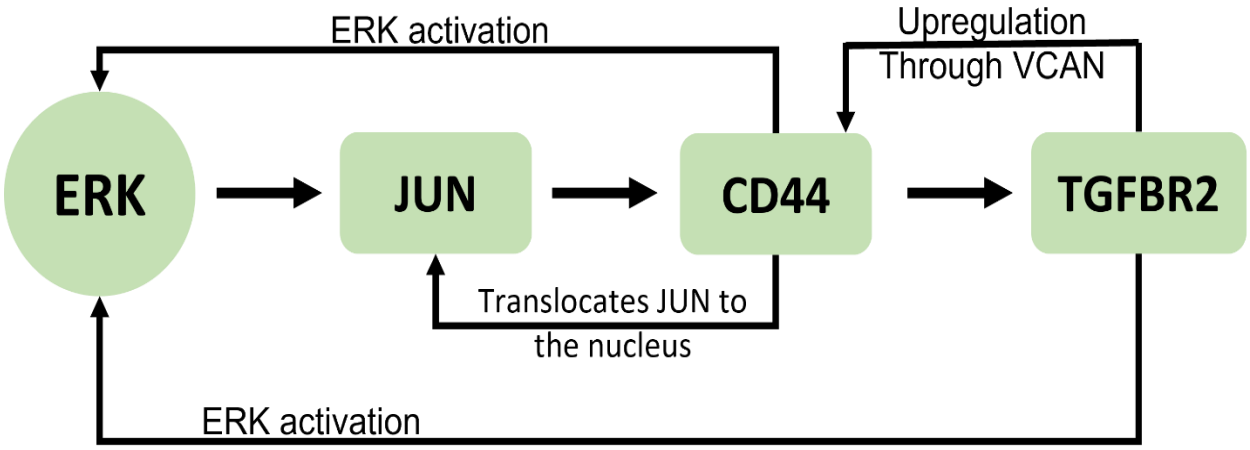

Figure 4. Schematic representation of how the most influential nodes JUN, CD44 and TGFBR2, of the CL gene upregulated network, affect and interact with each other showcasing their association with ERK pathway.

4.2 ERK Pathway and its involvement in the network

Cancer cells infiltrate and grow outside the tumour microenvironment before entering the circulatory system and migrate to neighbouring organs to proliferate and form a primary tumour (Pommier et al., 2020). To facilitate such a complex process, multiple signalling pathways are required to be coordinated. An important pathway that is proposed to mediate tumourigenesis in TNBCs is the activated Extracellular signal-regulated kinase 1/2 (ERK1/2), thought to be a prime oncogenic event for the formation of CL (Pommier et al., 2020) (Bhatt et al., 2021). Many diseases including cardiovascular, inflammatory, and neurodegenerative disorders as well as cancers, are attributed to the dysregulation of protein kinase signalling (Roskoski, 2019). Estimating that approximately 20–33% of all drug discovery programs target protein kinases, highlights their importance in various pathogenesis (Roskoski, 2019). These enzymes catalyze the following reaction:

$$\mathrm{MgATP^{1-} + protein\text{–}O{:}H \rightarrow protein\text{–}O{:}PO_3^{2-} + MgADP + H^+}$$

Enzymes are classified as either protein-tyrosine or protein-serine/threonine kinases depending on the substrate with which they interact. Dual-specificity protein kinases, such as MEK1/2, which can phosphorylate both tyrosine and threonine in the activation segment of ERK1/2, constitute a small group of these enzymes. Despite their unique ability to interact with both substrates, they are still considered protein-serine/threonine kinases based on their evolutionary development (Roskoski, 2019).

Description of the ERK pathway

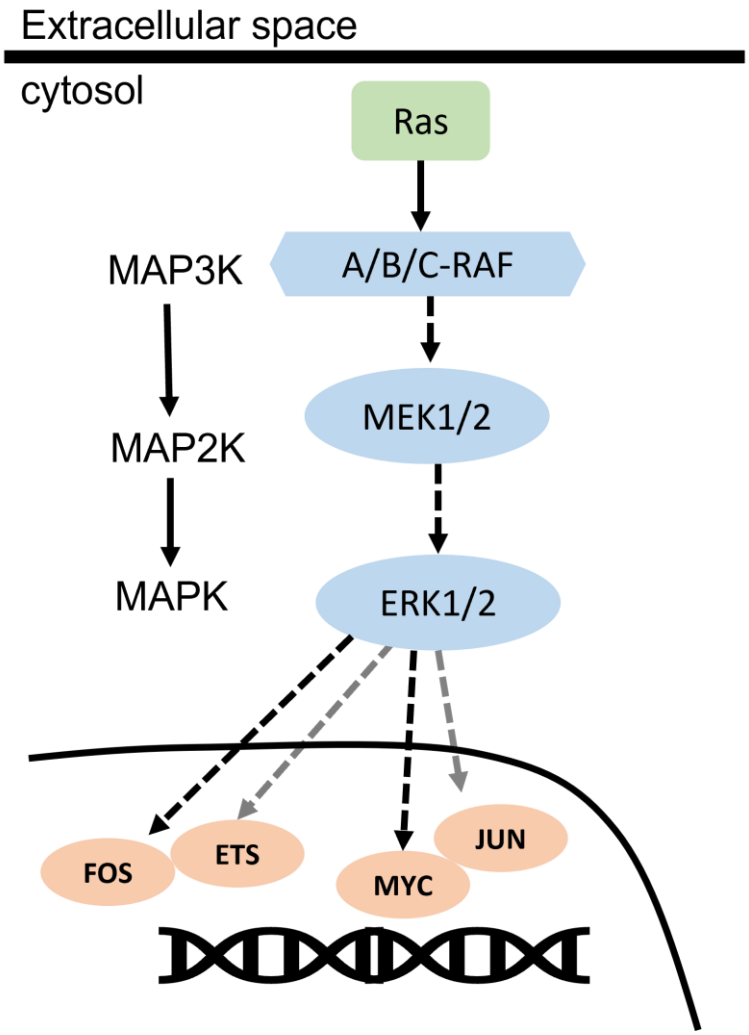

Figure 5. Schematic representation of the evolutionarily conserved Ras-Raf-MEK-ERK MAP kinase pathway.

The Raf enzymes, which are a type of protein-serine/threonine kinases, facilitate the phosphorylation and activation of MEK1 and MEK2, both of which are referred to as MAP/ERK Kinases. Consequently, MEK proteins then phosphorylate and activate ERK1 and ERK2, which belong to the family of Extracellular Signal-Regulated protein Kinases (ERK). Due to their narrow substrate specificity, the A/B/C-Raf enzymes and MEK1/2 can only interact with a limited range of substrates. Therefore, MEK1/2 are only known to act upon ERK1/2, and Raf enzymes only have MEK1/2 as their substrates (Roskoski, 2019)

ERK1/2 belongs to the mitogen-activated protein kinase (MAPK) family, which plays a role in signalling cascades and transmits extracellular signals to intracellular targets.

Basic processes like cell proliferation, differentiation and stress responses are regulated by central intracellular signalling elements like the MAPK cascades. The MAPK layer consists of four cascades: ERK1/2, c-Jun N-terminal kinase (JNK), p38 MAPK and ERK5. The first cascade regulates cell metabolism and function, by activating through phosphorylation, various transcription factors, when transferred to the nucleus, such as proto-oncogene c-Fos, proto-oncogene c-Jun, ETS domain-containing protein Elk-1, proto-oncogene c-Myc and cyclic AMP-dependent transcription factor ATF2 (**fig5.**) (Buonato & Lazzara, 2014). To decrease the metastatic properties of cancer it is proposed to activate the reverse, mesenchymal to epithelial transition (MET). Evidence shows that activation of the ERK1/2 and ERK5 pathways mediate EMT, the inhibition of those, found to promote MET which should additionally inhibit cellular proliferation, may mitigate risks associated with proliferation of micro-metastases (Buonato & Lazzara, 2014).

JUN

JUN expresses the transcription factor c-jun, an important component of the AP-1 complex, which plays a crucial role in gene regulation by binding to promoters of various genes, including CD44. More specifically, Lamp et al. (1997) showed that AP-1-directed increased expression of CD44 is necessary to mediate fibroblast invasion. Along with controlling gene expression, the AP-1 family is also shown to have an impact on cancer cell migration and invasion through angiogenesis. The relationship between c-jun activation and distant metastasis of breast cancer was proposed in vivo, for the luminal A subtype (Gee et al., 2000).

C-Jun transcription is also upregulated by its own product, as its promoter region contains high affinity binding sites for the AP-1 complex (Angel et al., 1988). However, JUN's activity is tightly controlled, and is suggested to be modulated by both transcriptional and post-translational modifications (Nam et al., 2015). For instance, the JNK pathway, once activated by a variety of extracellular stimuli such as stress cytokines, phosphorylates and activates c-Jun N-terminal kinases. The c-Jun N-terminal kinases (JNKs), are identified as kinases that activate JUN by phosphorylating Ser-63 and Ser-73 within its transcriptional activation domain (Kayahara et al., 2005). Similarly to ERK1/2, activated JNKs are involved in processes, including proliferation, differentiation, apoptosis, and survival, by acting on associated substrates (Papa et al., 2019).

ERK pathway also acts as a *JUN* regulator, since the pathway`s activation increases the expression and stability of *JUN* (Brennan et al., 2020). This process further enhances the regulatory function of AP-1 in controlling gene expression, cellular proliferation, and differentiation. Additionally, ERK can also indirectly regulate the AP-1 pathway by targeting other proteins that modulate AP-1`s activity, such as c-Fos and Elk-1 (Roskoski, 2019). Therefore, ERK plays a pivotal role in regulating the function of the AP-1 complex,

and its downstream targets. Thus, understanding the intricate regulatory mechanisms of c-Jun is crucial to better understand the impact of the AP-1 family on cellular and biological activities, including cancer.

CD44

The *CD44* gene encodes for a transmembrane glycoprotein that plays a crucial role in cell-cell and cell-matrix interactions. The primary binding partner for CD44 is hyaluronic acid (HA), a prevalent substance found in the extracellular matrix (ECM) produced by both stromal and cancer cells (Banerjee et al., 2016). HA attaches to the CD44 ligand binding domain, prompting structural alterations that facilitate the attachment of adaptor proteins or cytoskeletal components to inner cellular regions. This, in turn, triggers the activation of diverse signaling pathways, ultimately influencing cell proliferation, adhesion, migration, and invasion (Nam et al., 2015). Such pathways involve the stimulation of receptor kinases like Erb2n, EGFR, and TGF-beta receptors (Bourguignon & Chen, 2014). TGF-beta for example, was found to upregulate *Versican* (*VCAN*) in ovarian cancer, increasing its aggressiveness (Yeung et al., 2013). VCAN is a chondroitin sulfate proteoglycan known to form structural aggregations of HA. Moreover, VCAN upregulation was shown to upregulate the expression of *CD44* and *receptor of hyaluronic acid-mediated motility (RHAMM)*, leading to enhanced motility and invasion of ovarian cancer cells (Yeung et al., 2013).

ERK pathway was found to be activated by CD44, by interacting with growth factors and integrins, promoting their downstream signaling. Activation of the ERK pathway can in turn stimulate the phosphorylation/activation of CD44, which has been shown to enhance its binding to hyaluronic acid (Judd et al., 2012). Furthermore, ERK activation has been linked to increased secretion of matrix metalloproteinases (MMPs) (Tanimura et al., 2003). MMPs can degrade type 1 collagen and release collagen-derived peptides that are shown to increase the expression of hyaluronic acid synthase mRNA (Zhao et al, 2021). This hyaluronic acid increase can enhance its own signaling, promoting cell migration and invasion (Zhao et al, 2021).

Notably, Bourguignon & Chen (2014) reported that CD44-HA interaction is closely associated with JNK and c-Jun activation in TNBC cell line MDA-MB-468. The CD44-HA interaction was observed to promote the translocation of JUN to the nucleus (Bourguignon & Chen, 2014). Then, JUN can interact with an upstream/enhancer region, containing AP-1 binding sites, of the *miR-21* promoter, upregulating *miR-21*`s expression (Bourguignon & Chen, 2014). The overexpressed *miR-21* in turn positively contributes to the expression of genes *Bcl2, ABCB1* and *IAP*. Resulting in MDA-MB-468 cells acquiring anti-apoptosis/survival and chemoresistance properties (Bourguignon & Chen, 2014). Therefore, CD44's interaction with HA, and the downstream activation of the ERK pathway play an important role in cancer cell migration and invasion.

TGFBR2

TGFBR2 (Transforming growth factor, beta receptor II) encodes a member of the serine/threonine protein kinase family and the TGFB receptor subfamily. Physiologically, in normal and premalignant cells TGF-beta stimulates cytostasis and apoptosis, showing tumour suppression capabilities (Hao et al., 2019). However, with cancer progression, TGF-Beta transforms to tumour promoter by stimulating tumour cells to undergo the EMT (Hao et al., 2019). Both TGF-β-induced cell cycle arrest and EMT were shown to be facilitated by the ERK pathway (Principe et al., 2017). Cancer cells, during their transformation, get resistant to TGF-β-induced growth arrest, by their acquired mutations (Hao et al., 2019). However, while TGF-β and ERK appear to diverge with respect to the cell cycle arrest, ERK still drives TGFβ-induced EMT (Principe et al., 2017). TGF-β receptors directly phosphorylate ShcA on serine and tyrosine to induce its complex formation with Grb2/Sos (Lee et al., 2007). The resulting complex converts Ras into its active GTP-bound form, ultimately leading to the sequential activation of c-Raf, MEK and ERK1/2 (Lee et al., 2007).

The data suggests a positive regulation chain reaction between JUN, CD44 and TGFBR2, primarily through the activation of ERK pathway (**fig4.**), which is a shared effect in all three nodes. The influential nodes and their suggested interactions will be used as a reference for the rest of the results. This reference will be used to verify their possible effect/linkage to CL via associations to its genetic signature, while trying to interpret their possible mechanism of action.

4.3 Disease areas covered in the drug lists

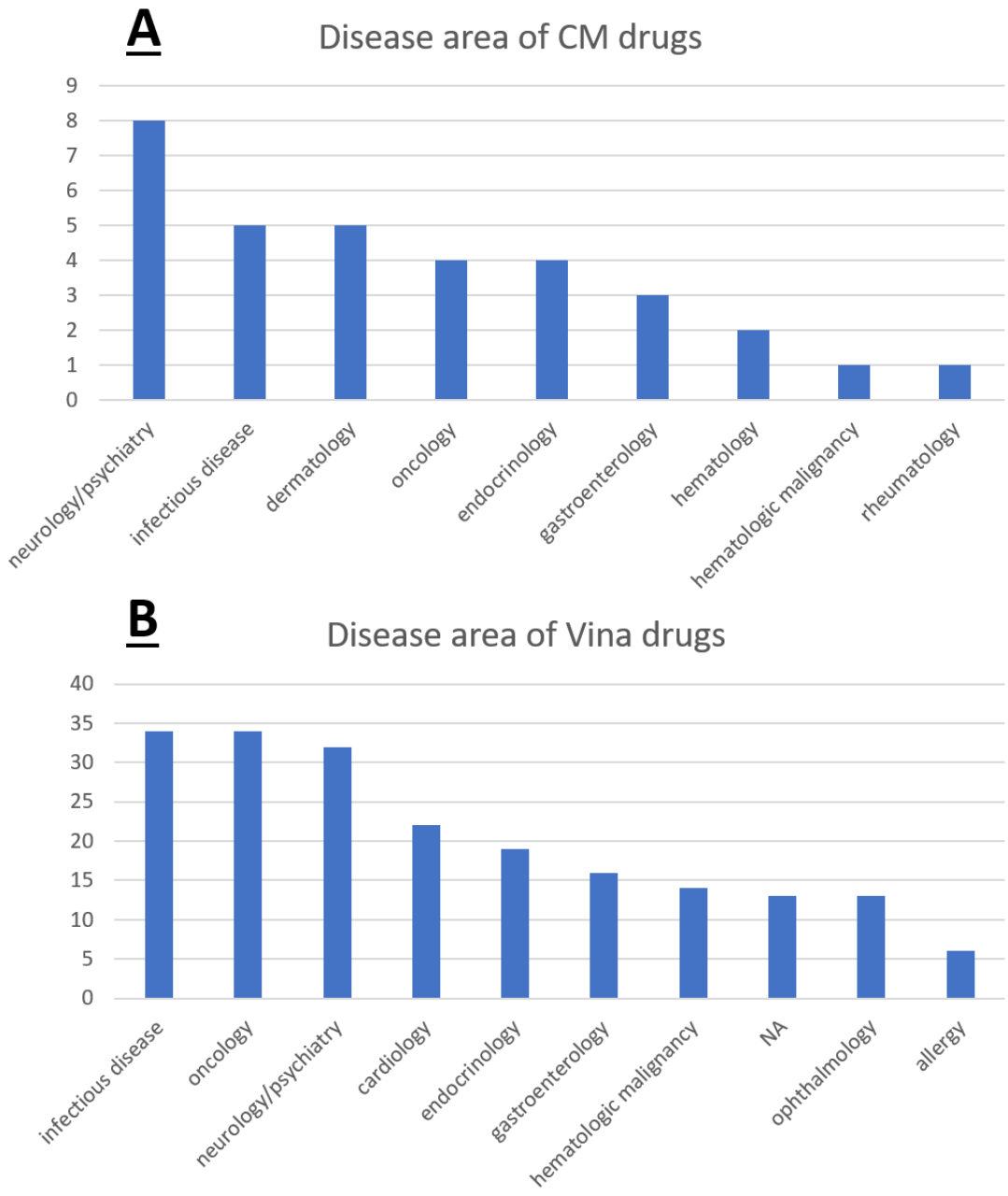

Figure 6. A) The grouping of the CM FDA approved compound list, consisting of 38 entries. B) The grouping of the Autodock Vina compound list of 203 FDA approved drugs.

After gaining more theoretical understanding, the upregulated signature of CL was analyzed in Connectivity Map (CM) query.io tool to determine a list of compounds able to reverse it. In addition, a structural analysis was conducted for ANPEP protein to

determine compounds able to physically interact and inhibit its action. ANPEP is associated with metastasis on a broader level, as it is found to be overexpressed in a variety of cancers, while the CM analysis will provide more specific results associated with the metastatic ability and phenotype of CL. The CM and Vina compound lists of FDA approved molecules were grouped based on their respective disease area. Both lists show that the majority of them are found in the common groups, infectious diseases, psychiatry, endocrinology, oncology and gastroenterology (**fig6.**). From the CM analysis, a drug list specific to the MCF7 cell line was isolated, as it is taken from the epithelial cells of breast tissue with metastatic adenocarcinoma and is the most widely used line in breast cancer (Lee et al., 2015). Dermatology and ophthalmology refer to compounds for external application, so they were excluded from further analysis. Furthermore, oncology refers to compounds already used as cancer treatments, and although they may be potential soft repurposing candidates, their mechanism of action is already characterized.

Neurology

The psychiatry/neurology disease area is known to be associated with oncology, as both cancer and neurodegenerative disorders are attributed to dysregulated protein kinase signaling (Roskoski, 2019). JNKs, previously referred for their role in JUN regulation, are also found to be overexpressed in patients with Alzheimer's disease. More specifically, JNK3 is correlated with the rate of cognitive decline, as found overexpressed and activated in brain tissue (Ramon Yarza, 2016). Moreover, the gene ANPEP was found to be overexpressed in Parkinson's disease (PD) cases compared to control subjects (Lowes et al., 2020). Interestingly, ANPEP levels were also significantly elevated in prodromal individuals compared with healthy control subjects (Lowes et al., 2020). Elevated ANPEP expression is a characteristic feature of inflammation and has been detected in neurodegenerative conditions. Decreasing its function has been explored as a potential treatment for reducing inflammation (Lowes et al., 2020).

Infectious diseases

Infectious diseases refer to compounds like antibiotics. There is evidence regarding their applications in cancer, showing anti-proliferative and pro-apoptotic capabilities. Anticancer antibiotics are able to inhibit the proliferation of cancer cells by killing them in all stages of proliferation, even cells in G0 stage, which are often omitted by conventional anticancer drugs (Gao et al., 2020). Furthermore, anticancer antibiotics were shown to promote apoptosis by targeting the *pro survival B cell lymphoma-2 (Bcl-2)*, *apoptotic pro-Bcl-2-associated x (Bax)*, caspase-3/8/9 and P53 (Gao et al., 2020). Beberok et al. (2018) reported that ciprofloxacin inhibition of the Bax/Bcl-2-dependent pathway induces apoptosis in human TNBC MDA-MB-231 cells, by the loss of the mitochondrial transmembrane potential. Moreover, combination of the antibiotics metformin and salinomycin was shown to inhibit EMT induced cell migration by blocking the tumour

growth factor (TGF), in non-small cell lung cancer (NSCLC) cell lines (Sánchez-Tilló et al., 2014).

Endocrinology

TNBC is a subtype of breast cancer known not to be influenced by estrogen or progesterone hormones. Consequently, traditional endocrine therapies targeting these hormones are not effective in treating TNBC. However, there is growing interest in an alternative receptor known as androgen receptors (AR) that could potentially serve as a target for therapeutic interventions (Lacopetta et al., 2012). Although primarily associated with prostate cancer, androgen receptors are also found in breast cancer cells, including TNBC. Ongoing clinical trials have provided evidence suggesting that patients with AR-positive luminal-type (LAR) TNBC may derive benefits from anti-androgen drugs commonly used in the treatment of prostate cancer (Lacopetta et al., 2012). These findings have sparked interest in exploring the potential of targeting androgen receptors as a viable therapeutic strategy for TNBC patients who do not respond to traditional endocrine therapies.

Gastroenterology

The efficiency of most breast cancer treatments is usually impaired by limitations like cytotoxicity and the emergence of drug resistance. For example, invasiveness and chemoresistance are conferred by a common feature of tumour cells, the surrounding acidic environment. Proton pump inhibitors (PPIs) function by blocking the secretion of gastric acid through the inhibition of the H+/K+-ATPase enzyme in parietal cells. They are widely used as drugs of choice for the treatment of acid-related conditions, like the gastroesophageal reflux disease (GERD) (Joo et al., 2019). PPI examples like lansoprazole, omeprazole, and Pantoprazole were shown to inhibit the growth of MDA-MB-231, MCF7, and T47D breast cancer cells, through apoptosis induction (Ihraiz et al., 2020). More specifically, in MDA-MB-231 cells, PPIs treatment also significantly inhibited cell migration (Ihraiz et al., 2020).

4.4 Evaluation and selection of the shared drugs among the lists

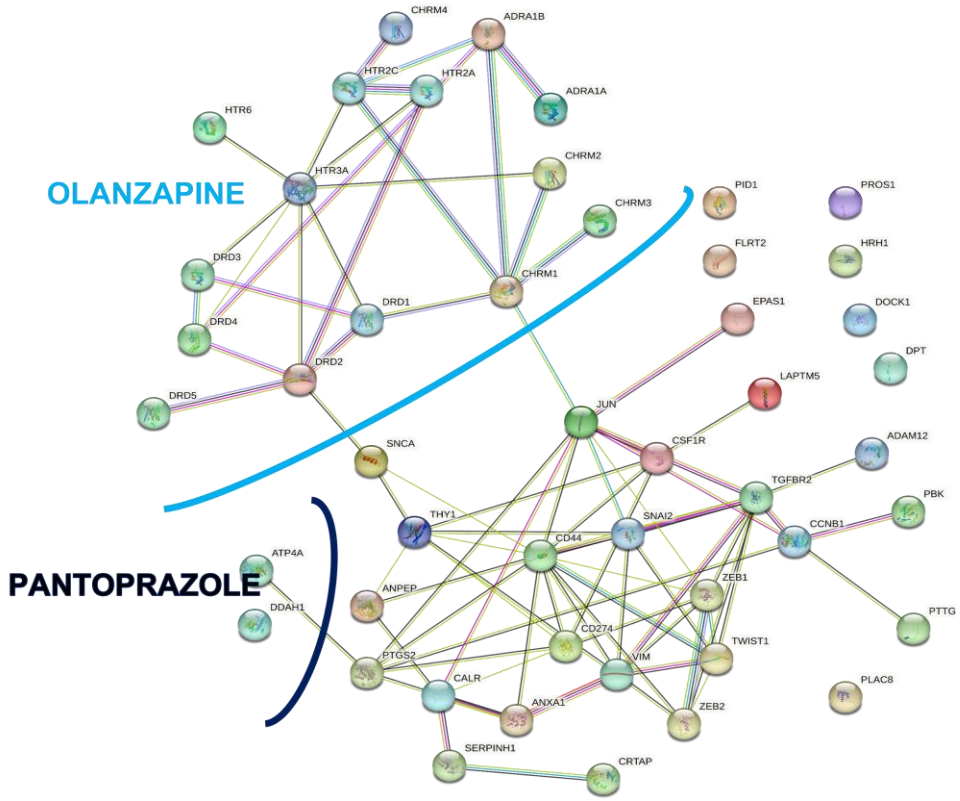

Figure 7. The genes targeted by Pantoprazole and Olanzapine were added to the CL genetic signature network to determine possible associations.

CM analysis generated a list of 38 compounds taking into account the summary of six different cell lines. The procedure was repeated considering only the cell line MCF7, which is widely used in breast cancer research, showing a total of 66 potential compounds. The docking analysis of ANPEP generated a list of 204 compounds, setting a threshold of the affinity score of the known FDA-approved ANPEP-inhibitor compound Ezetimibe, showing 30 heavy atoms and binding affinity of -9.713. The drugs appearing in all three lists were identified to further narrow down to the most promising repurposing candidates. The common compounds were identified to be GOSERELIN, LAPATINIB, PANTOPRAZOLE, and OLANZAPINE. The first two of them are antineoplastic and they are already used in breast cancer, showing no soft-repurposing value. More specifically, Lapatinib is an antineoplastic medication used in the treatment of advanced or metastatic HER-positive breast cancer. Goserelin, on the other hand, is a synthetic analog of luteinizing hormone-releasing hormone, primarily employed in the management of breast cancer and prostate cancer.

Pantoprazole

As a proton pump inhibitor (PPI), Pantoprazole functions by blocking the secretion of gastric acid through the inhibition of the H+/K+-ATPase enzyme in parietal cells. The network in **fig7** shows a connection between the Pantoprazole target ATP4A and the CL gene PTGS2. ATP4A and ATP4B subunits of the gastric proton pump were detected in the larynx of patients with laryngeal squamous cell carcinoma (McCormick et al., 2021). McCormick et al. (2021) research supports the contribution of laryngeal-expressed H+/K+ ATPase to local inflammation and carcinogenesis. More specifically, increased expression of inflammation and laryngeal cancer-related genes, such as IL1B, PTGS2, and TNFA, was shown because of the ectopic expression of the proton pump (McCormick et al., 2021). When gastric H+/K+ ATPase was expressed in hypopharyngeal cells, it led to mitochondrial damage through cristae degradation. However, no evidence of mitochondrial damage or alterations in gene expression was observed when only a single subunit was expressed, suggesting that the secretion of acid by functional proton pumps in the upper airway mucosa could induce local cellular and molecular changes associated with inflammation and cancer (McCormick et al., 2021).

Several studies have suggested that Pantoprazole (PPZ) has the potential to inhibit the progression of TNBC by inducing cell cycle arrest and apoptosis, as reported by Ihraiz et al. (2020) and Goh et al. (2014). Yeo et al (2008) hypothesized that PPIs are possible to induce apoptosis in gastric cancer (GC) cells, as pre-treatment with PPI resulted in total inhibition of ERK1/2. Later, Feng et al. (2016) showed that Pantoprazole was able to decrease the relative expression levels of stem cell markers, including *CD44*, known to possess a crucial role in cancer initiation, progression, recurrence, and resistance to chemotherapy. Cancer stem cells (CSCs) have the ability to self-renew and differentiate into multiple cell types, thus contributing to tumour development. Traditional chemotherapies primarily target the bulk of cancer cells, leaving behind CSCs that can lead to tumour relapse (Gupta et al., 2009). Feng et al. (2016) study indicates that the treatment with PPZ enhances the chemosensitivity of cells, potentially targeting CSCs and reducing their sphere-forming ability and expression of stem cell markers. In the context of CSCs, it is important to highlight the involvement of two key signaling pathways: epithelial-to-mesenchymal transition (EMT) and Wnt/β-catenin signaling. These pathways are known to contribute to the stemness of CSCs. EMT, in particular, plays a significant role in promoting CSC formation in various solid tumours. It is associated with the upregulation of stem cell-related transcription factors and an increase in tumourigenic potential (Lichner et al., 2015).

It was observed that the treatment of spheres with PPZ resulted in the inhibition of EMT progression and the suppression of β-catenin activation to some extent (Feng et al., 2016). These findings indicate that PPZ exerts its antitumour effects by targeting CSCs

through the EMT/β-catenin signaling pathways. This suggests that PPZ may disrupt the mechanisms that maintain CSC stemness and contribute to tumour progression. Furthermore, Pommier et al. (2020) reported that the activation of the RAS/MAPK pathway is a recurring feature in CL breast cancers, and certain subsets of these cancers that possess stem cell characteristics exhibit exceptionally high RAS signaling. This highlights the importance of the RAS pathway in claudin-low breast cancer and its association with stem cell features. Understanding the intricate interplay between signaling pathways, such as EMT, Wnt/β-catenin, and RAS/MAPK, in regulating CSCs is crucial for developing targeted therapies that can effectively eliminate CSCs and improve patient outcomes (Feng et al., 2016).

Olanzapine

Olanzapine is an antipsychotic drug that acts as an antagonist for various neuronal receptors like the dopamine (DRD) and serotonin receptors (5-HT). Downregulation of DRD2 and 5-HT_2A receptor activities were found beneficial in cancer chemotherapeutics. In addition, inhibition of DRD4 has been shown to reduce cellular migration in breast cancer cells, although the mechanisms remain unclear (Rosas-Cruz et al., 2022).

Olanzapine targets two receptors that appear to be associated with the CL network, CHRM1 and DRD2, which interact with JUN and SNCA, respectively (**fig7.**). The CHRM1 receptor is a G protein-coupled receptor that activates intracellular signaling pathways when bound by acetylcholine (Calaf et al., 2022). The downstream signaling pathways of CHRM1 receptors are diverse and include the MAPK/ERK signaling pathway, which is responsible for JUN activation. Therefore, it is possible that Olanzapine-mediated regulation of CHRM1 expression could indirectly affect the activity of JUN and the MAPK/ERK signaling pathway (Calaf et al., 2022).

Regarding the interaction between DRD2 and SNCA, there is currently no clear information available. In an experiment, conducted by Filatova et al. (2017), targeting the GABA alpha receptors of neuroblastoma IMR-32 cells with Olanzapine and the anxiolytic peptide selank, showed that the mRNA of *SNCA* was found significantly increased. On the other hand, the most significant decrease in expression was observed in the genes *CSF2* and *JUNB* (Filatova et al., 2017). More specifically, the observed decrease was 6.3 and 6.7 times after incubation with the same compounds (Filatova et al., 2017). JUNB is an AP-1 family member, found to have both an antagonistic and compensatory relation with c-Jun (Novoszel et al., 2021). Finch et al. (2002) showed that by decreasing the expression of JUNB in malignant mouse keratinocytes, the activity of AP-1 was increased, resulting in a positive effect on tumour cell proliferation.

4.5 Gene Ontologies of the genes targeted by the drug lists

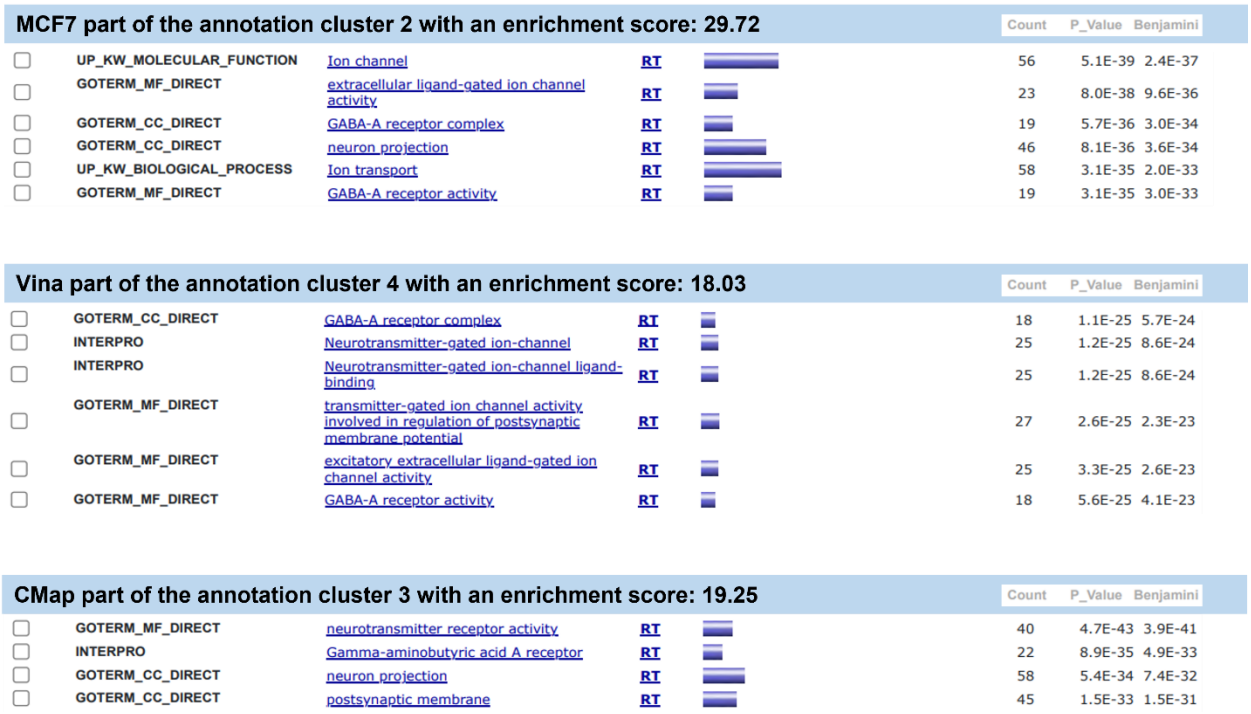

MCF7 part of the annotation cluster 2 with an enrichment score: 29.72				Count	P_Value	Benjamini
UP_KW_MOLECULAR_FUNCTION	Ion channel	RT		56	5.1E-39	2.4E-37
GOTERM_MF_DIRECT	extracellular ligand-gated ion channel activity	RT		23	8.0E-38	9.6E-36
GOTERM_CC_DIRECT	GABA-A receptor complex	RT		19	5.7E-36	3.0E-34
GOTERM_CC_DIRECT	neuron projection	RT		46	8.1E-36	3.6E-34
UP_KW_BIOLOGICAL_PROCESS	Ion transport	RT		58	3.1E-35	2.0E-33
GOTERM_MF_DIRECT	GABA-A receptor activity	RT		19	3.1E-35	3.0E-33

Vina part of the annotation cluster 4 with an enrichment score: 18.03				Count	P_Value	Benjamini
GOTERM_CC_DIRECT	GABA-A receptor complex	RT		18	1.1E-25	5.7E-24
INTERPRO	Neurotransmitter-gated ion-channel	RT		25	1.2E-25	8.6E-24
INTERPRO	Neurotransmitter-gated ion-channel ligand-binding	RT		25	1.2E-25	8.6E-24
GOTERM_MF_DIRECT	transmitter-gated ion channel activity involved in regulation of postsynaptic membrane potential	RT		27	2.6E-25	2.3E-23
GOTERM_MF_DIRECT	excitatory extracellular ligand-gated ion channel activity	RT		25	3.3E-25	2.6E-23
GOTERM_MF_DIRECT	GABA-A receptor activity	RT		18	5.6E-25	4.1E-23

CMap part of the annotation cluster 3 with an enrichment score: 19.25				Count	P_Value	Benjamini
GOTERM_MF_DIRECT	neurotransmitter receptor activity	RT		40	4.7E-43	3.9E-41
INTERPRO	Gamma-aminobutyric acid A receptor	RT		22	8.9E-35	4.9E-33
GOTERM_CC_DIRECT	neuron projection	RT		58	5.4E-34	7.4E-32
GOTERM_CC_DIRECT	postsynaptic membrane	RT		45	1.5E-33	1.5E-31

Figure 8. Functional annotation clustering of all the genes targeted by the compounds of the three different drug lists MCF7/Vina/CM. The analysis showed that ontology terms regarding Receptors and ion channels are shared among cluster 2 of MCF7, cluster 4 of Vina, and cluster 3 of CM. The most specific term appeared is the GABA alpha-receptor activity.

The three compound lists were processed to determine all genes that are targeted by the compounds. Then, DAVID functional annotation clustering was employed to determine the gene ontology terms of those genes. The first cluster of all three analyses is associated with kinases and protein phosphorylation, known to be key procedures targeted in cancer, and cardiovascular, inflammatory, and neurodegenerative disorders. The second most common cluster among them is related to transmembrane proteins (receptors) that allow ion transportation, in response to ligand binding. The common clusters in the gene ontology analysis show GABA alpha receptor (GABAAR) activity as the most specific term, enriched in all sets of genes (**fig8.**). The fact that the term also appears in the list of ANPEP suggests that affecting GABAAR activity may be of broader interest for cancer treatment, than just reversing CL signature.

4.6 GABA receptor and its association with ERK pathway

The MAPK pathway is implicated as a negative modulator of GABAAR function, and it may have an impact on GABA-gated currents via phosphorylation of the alpha subunit (Bell-horner et al., 2006). The GABAAR is a ligand-gated ion channel whose activity and function can be controlled either directly by ligand binding or indirectly by the phosphorylation of certain subunits that make up the receptor´s pentamer. The alpha subunit's function as a pertinent target of signalling kinases is largely unclear, even though the majority of studies on phosphorylation have concentrated on either beta or gamma subunits.

When GABA molecules or similar substances bind to the receptor and trigger its activation, the channel briefly opens, enabling the movement of ions, like chloride ions (Cl^-), from outside the cell to its interior (Bhattacharya et al., 2021). Benzodiazepines, like diazepam, are positive allosteric modulators of the receptors and act to enhance movement of chloride anions when GABA is bound to the receptor (Bhattacharya et al., 2021). GABA, a neurotransmitter, exhibits widespread distribution in various tissues throughout the body. Expression of GABAAR subunits, which form the GABA receptor, has been observed in diverse tissues including lung, pancreas, kidney, intestine, prostate, testis, ovary, liver, thyroid, and skin (Bhattacharya et al., 2021). Previous studies have emphasized the significance of GABA signaling in cellular processes such as proliferation, migration, and differentiation (Leonzino et al, 2016). Notably, GABA and GABAAR may play crucial roles in the immune system and stem cell development, which could be linked to their importance in cancer biology. More specifically, GABA signaling, whether through autocrine or paracrine mechanisms, exerts an inhibitory effect on the proliferation of embryonic stem (ES) cells and peripheral neural crest stem (NCS) cells.

Ion channels, including GABAAR, play crucial roles in regulating various physiological functions such as cellular excitability, ion homeostasis, and cell migration (Bhattacharya et al., 2021). Dysfunctions in ion channels are associated with disorders known as channelopathies. In the context of cancer, ion channels may contribute to invasive tumour metastasis and the development and progression of tumours (Bhattacharya et al., 2021). Rapidly proliferating cancer cells often exhibit a depolarized membrane potential compared to non-proliferating cells, which can drive cell proliferation (Yang & Brackenbury, 2013). GABAARs, like other ion channels, may contribute to the development and maintenance of cancers. Genes encoding subunits of GABAAR have been implicated in various types of cancers, including those of the central nervous system (gliomas, medulloblastoma, and neuroblastoma) as well as systemic cancers affecting the lung, breast, pancreas, liver, colon, prostate, thyroid, ovaries, and skin (Bhattacharya et al., 2021).

GABAAR in cancer

Enhanced expression of the *GABRA3* gene, responsible for the α-3 subunit expression of GABAAR, plays a crucial role in breast cancer, contributing to the migration and invasive characteristics of cancer cells (Bhattacharya et al., 2021). GABAARs containing the α-3 subunit activate Akt, a protein involved in regulating cell proliferation and migration in cancer cells (Bhattacharya et al., 2021). This increased activation of Akt may explain the heightened metastatic potential observed in breast cancer cells with elevated *GABRA3* expression. Moreover, the a-5 subunit was also shown to contribute to cancer growth, as knockdown of *GABRA5* reduced the growth of patient-derived medulloblastoma cells (Bhattacharya et al., 2021). In breast cancer, besides *GABRA3* and *GABRA5*, there is increased expression of the GABAAR subunit pi, encoded by the GABRP gene. This enhanced expression of GABRP is specifically observed in basal-like breast cancer (BLB-C subtype) (Sizemore et al., 2014). It is associated with metastases to the brain and correlates with a poorer prognosis for patients. Mechanistically, GABAAR containing the pi subunit seems to play a role in maintaining the expression of basal-like cytokeratins, phosphorylation and activation of ERK1/2 (Sizemore et al., 2014). In addition, Juvale et al. (2021) identified the overexpression of *γ-aminobutyric acid receptor subunit π (GABRP)* in circulating breast cancer cells. Particularly, patients with metastatic breast cancer were shown to express it eight times higher than in patients with no evidence of metastasis of stages II-IV (Juvale et al., 2021). When *GABRP* was overexpressed, there was a marked increase in cell migration and invasion, as well as an upregulation of MMP expression due to the activation of the ERK pathway. Moreover, Sung et al. (2017) observed that GABRP knockdown diminished the migration and invasion of SK-OV-3 cells and reduced ERK activation.

Kleinerman et al. (1984) first showed perturbing tumour formation and/or cancer proliferation by disrupting GABAergic signaling. In the 1984 study, a retrospective analysis of breast cancer patients and benzodiazepine usage (specifically diazepam) was conducted. The study revealed that the use of diazepam correlated with reduced primary tumour size and a lower incidence of lymph node involvement. One possible explanation is that patients who took diazepam experienced better outcomes due to the use of an anxiolytic agent that helped them cope with the anxiety associated with their condition (Bhattacharya et al., 2021). Alternatively, it is possible that the BC tumour cells or the cells within the tumour microenvironment were responsive to diazepam in a way that contributed to an anti-cancer effect. A series of benzodiazepine analogs, that bind to GABAAR, containing the GABRA5 subunit, were demonstrated to inhibit the viability of medulloblastoma cells in culture (Jonas et al., 2016). More importantly, Jonas et al. (2016) stated that “the effect *in vivo* was more significant and specific than standard-of-care chemotherapeutic”. In a follow up study, single-cell electrophysiology was conducted to determine the etiology of the impairment of medulloblastoma cells by benzodiazepines.

The benzodiazepines analogs tested, including diazepam, were found to cause depolarization of the mitochondrial membrane by inducing chloride anion efflux to the cells, resulting in mitochondrial fission (Kallay et al., 2019). In conclusion, GABAAR may indeed contribute to cancer development, as it is found to be overexpressed in many cancers. However, the significant chloride anion efflux resulting from benzodiazepine binding to GABAAR elicits a stress response (Kallay et al., 2019). As a result, it triggers an apoptotic reaction through the intrinsic (mitochondrial) pathway, which entails the activation of the pro-apoptotic protein BAD, known as the BCL2 associated agonist of death (Kallay et al., 2019)

4.7 ANPEP and its structural analysis

ANPEP functions as a zinc-dependent metalloproteinase, facilitating the breakdown of peptide bonds located at the N-terminal end of neutral residues. The enzymatic process of ANPEP is delineated as follows: Glu406, His383, and His387 bind with the Zn2+ ion, converting a water molecule into a catalyst; subsequently, a proton is transferred to Glu384, and ultimately, this proton is transferred to the nitrogen group of the protein (Qu et al., 2015). A tumour-inducing (carcinogenic) function of ANPEP that lies beyond its aminopeptidase activity, is its participation in tumour cell motility and adhesion (Datar et al., 2004). Stable expression of ANPEP on tumour cell surfaces greatly increases their migratory capacity (Mina-Osorio, 2008). Although the specificity for ANPEP is not well studied, knocking it out or using anti-ANPEP antibodies was shown to block tumour migration (Mina-Osorio, 2008). In Hepatocellular carcinoma (HCC), Zhai et al. (2020) showed that ANPEP phosphorylates the Branched chain ketoacid dehydrogenase kinase (BCKDK), which interacts and activates ERK1/2, suggesting that ANPEP may act as an indirect positive regulator of ERK pathway. The mechanisms whereby ANPEP mediates tumour migration have been partially linked to its aminopeptidase activity, as it was shown that it degrades extracellular matrix proteins. This suggests that neutral ANPEP plays a crucial role in matrix degradation and invasion by tumour cells and that its inhibitors may be useful for preventing the spread of malignant cells (Datar et al., 2004).

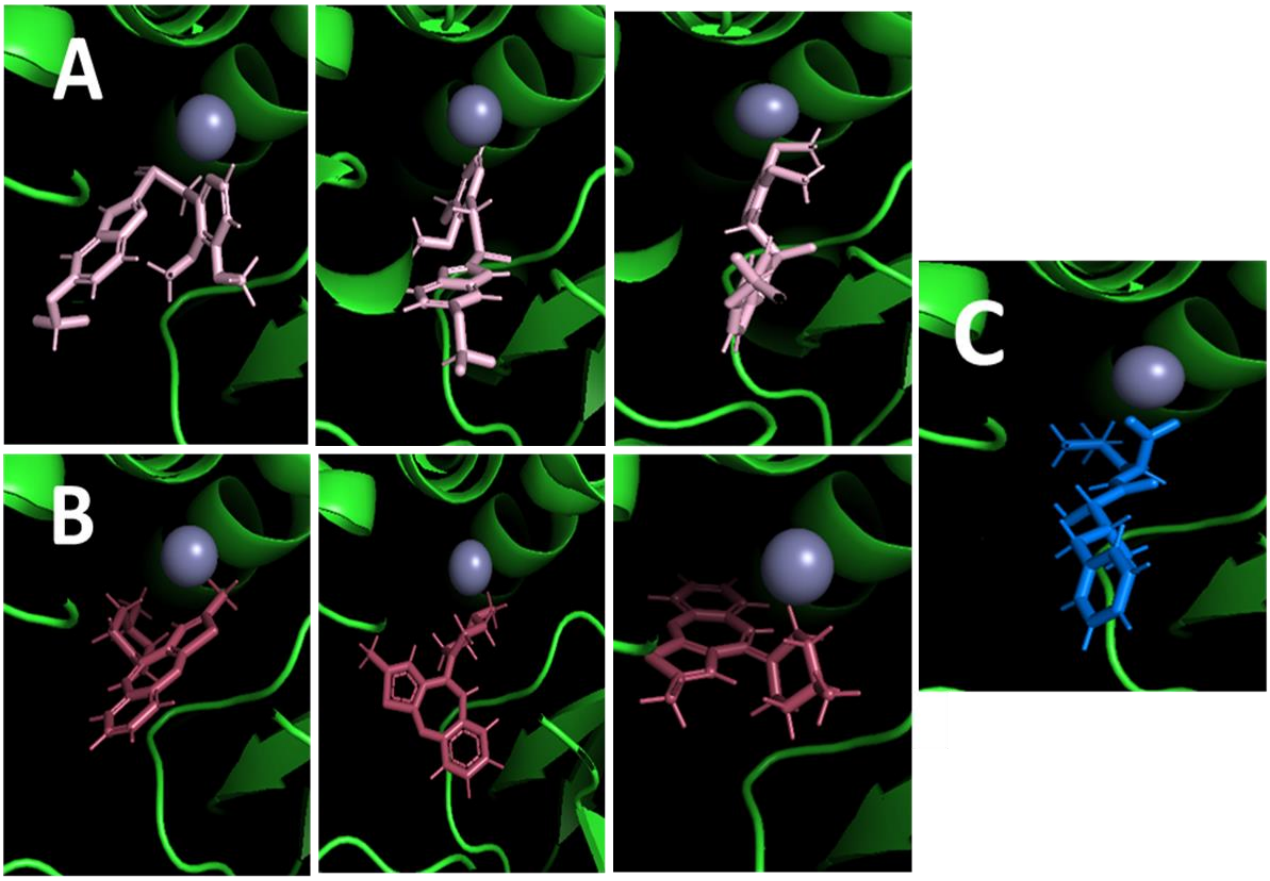

Figure 9. The panels show the active site of ANPEP protein (green), containing a Zinc ion (grey), complexed with different conformations of two shared drugs and an already characterised ligand. A) Shows the three different conformations of Pantoprazole in the active site of ANPEP. B) Shows three different conformations of Olanzapine to be tested with MD simulations. C) Finally, is the experimentally characterised complex of ANPEP with Bestatin (Blue).

The starting poses of Pantoprazole and Olanzapine, for the molecular dynamics simulations were selected from the Autodock Vina results (**fig9A-B.**). In addition, Bestatin is used as reference to compare the interactions of the ligands to the protein (**fig9C**.). Bestatin was found to form hydrogen bonds with Glu326, Gln150 and Tyr414, pi-pi interaction with Phe409, and metal interaction with the zinc ion (**fig10.**).

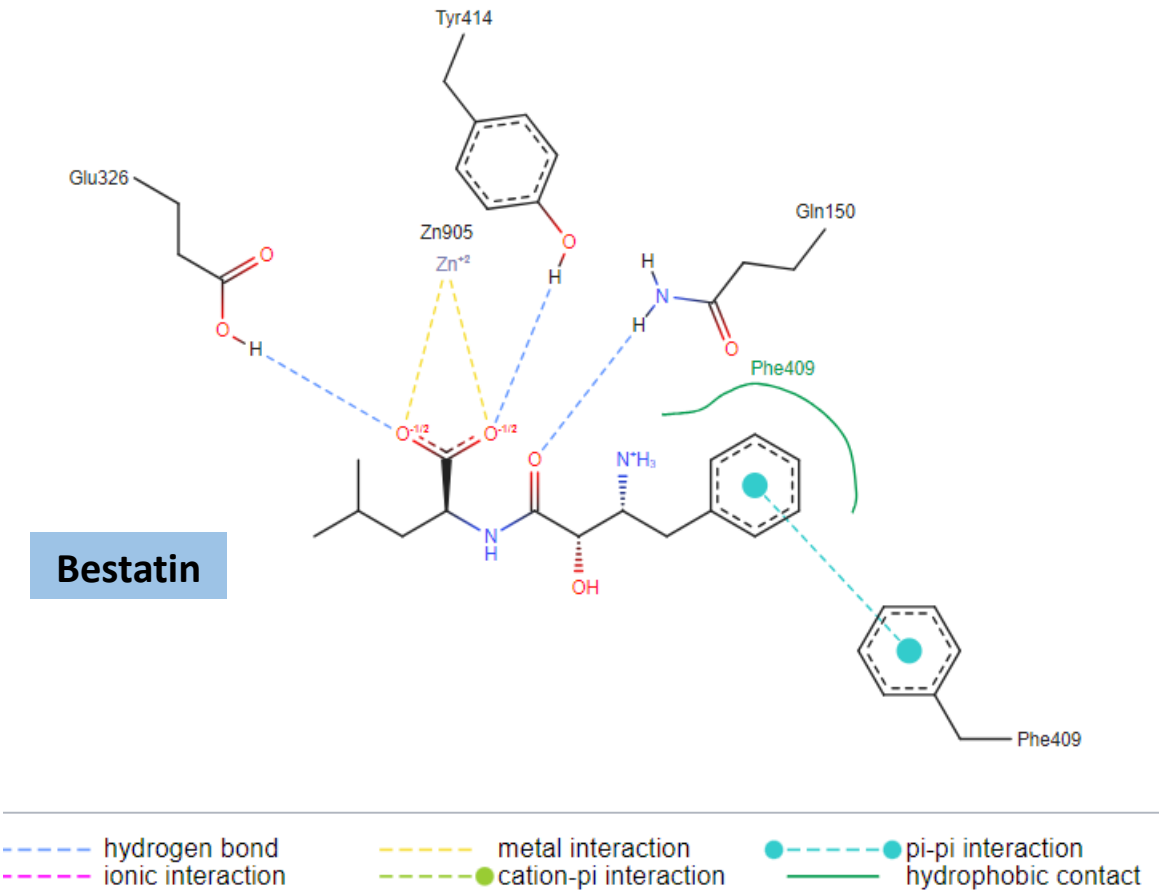

Figure 10. Shows the 2D representation, generated by the PoseView, of the interaction profile between the ligand Bestatin and the ANPEP protein.

The interaction profiles between the different conformations of the candidate ligands shown in **fig11** are described below: Panto02 forms pi-pi interactions with His325 and Phe409, and a hydrogen bond with Gln148. Panto10 forms three hydrogen bonds with Tyr414, Gln148, and Gln150. Panto15 forms a hydrogen bond with Ala290, a pi-pi interaction with Tyr414. The Pantoprazole conformations show to make pi-pi interactions, hydrogen bond, hydrophobic contacts, and metal interaction with the zinc ion. The Olan20 and Olan13 conformations don't form a metal interaction with the zinc ion. Olan13 forms a hydrogen bond with Ala290, pi-pi interactions with Tyr414 and His325, and finally an ionic interaction with Glu292. Olan20 forms a hydrogen bond with Gln150 and a pi-pi interaction with Phe409. All three conformations show hydrophobic contacts, with only Olan01 interacting with the zinc ion.

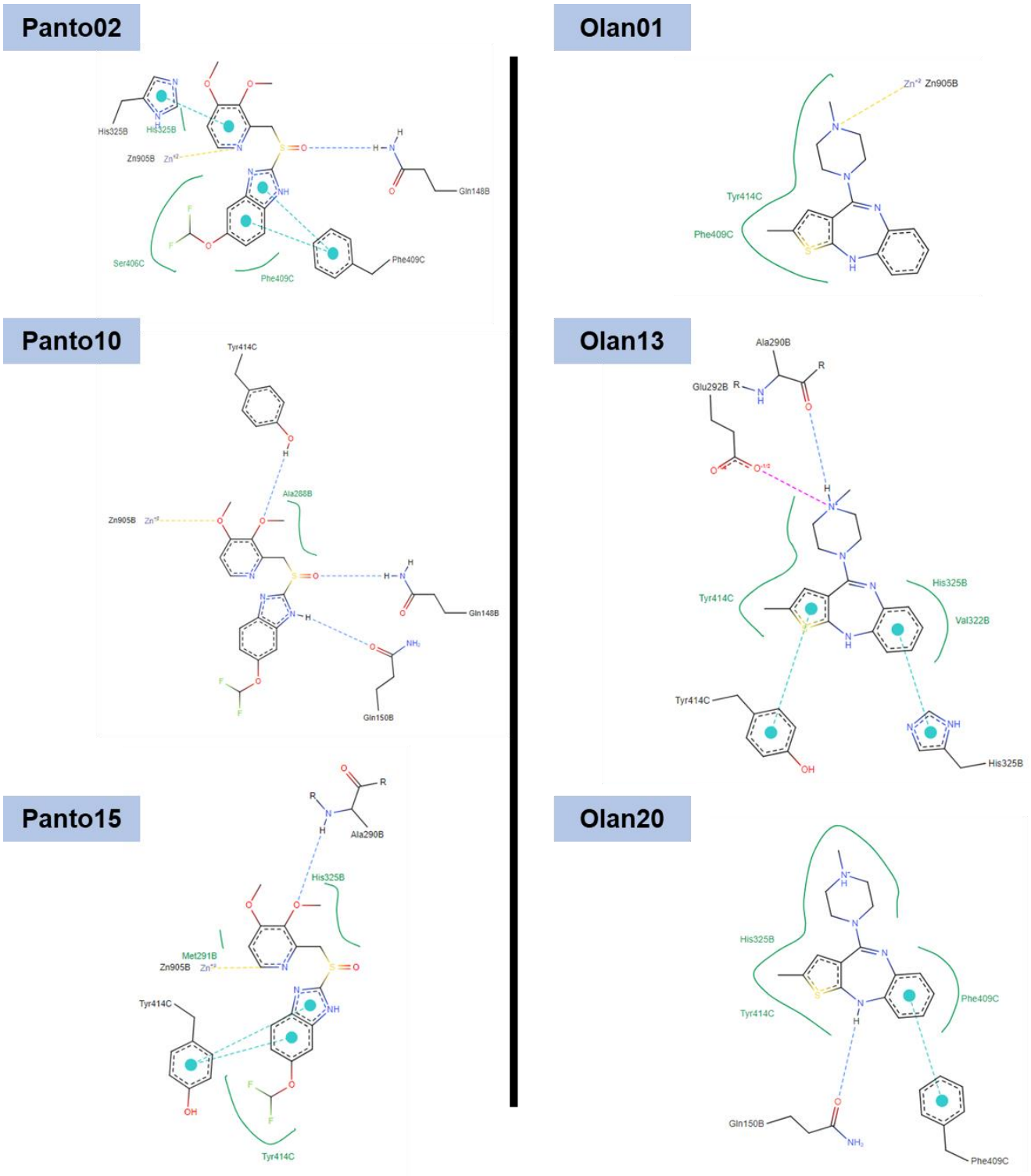

Figure 11. Graphical 2D representations of the interaction profile between, Pantoprazole conformations (left) and Olanzapine conformations (right), with the ANPEP protein.

Table 2. shows the respective residues that each ligand interacts with.

		Interacting Residue								
		Zn905	His325	Gln148	Phe409	Tyr414	Gln150	Ala290	Glu292	Gln326
Ligands	Bestatin	X			X	X	X			X
	Panto02	X	X	X	X					
	Panto10	X		X		X	X			
	Panto15	X				X		X		
	Olan01	X								
	Olan13		X			X		X	X	
	Olan20				X		X			

The 3D structure of the ANPEP protein represents its active and closed conformation. Bestatin is an already characterised inhibitor of the closed conformation. The rest of ligand conformations, with their interacting residues except of hydrophobic interactions, are shown in **table2**. Panto10 shows 60% percent residue interaction similarity with Bestatin, while Olan20 shows 40%. Apart from the active form, it has also been suggested that the inactive open conformation can also play a functional role by binding to the exposed N terminus of proteins that wouldn't be accessible to ANPEP in the closed conformation. The potential interaction of ANPEP's inactive form with extracellular matrix proteins and cell-surface proteins may confer unknown functions around cell motility and adhesion (Chen et al., 2012). This was tested by Chen et al. (2012) showing the interaction between ANPEP and TNF, and the possible inhibition of ANPEP by using ligands to compete with the exposed N terminus of TNF. In this concept, the distinct residue interactions of Olanzapine and Pantoprazole with ANPEP may unveil a different mode of inhibition.

ANALYSIS OF MOLECECULAR DYNAMICS

Bestatin

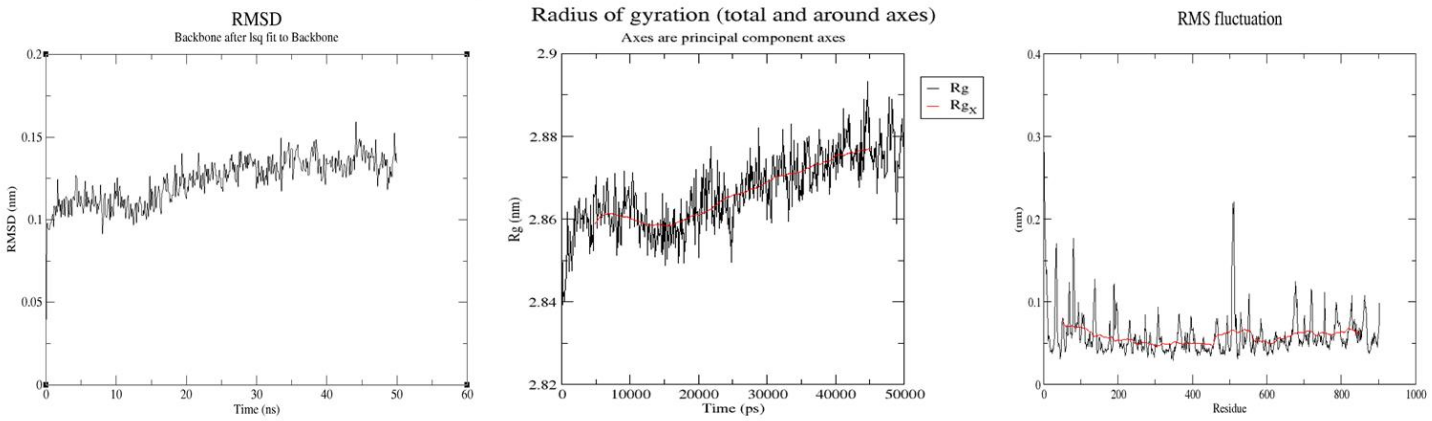

Figure 12. Three graphs generated from the molecular dynamics simulation of ANPEP-Bestatin complex for 50ns. Namely, (left) the Root-mean-square deviation (RMSD), (right) the root-mean-square fluctuation (RMSF), and (centre) the radius of gyration (rGyr).

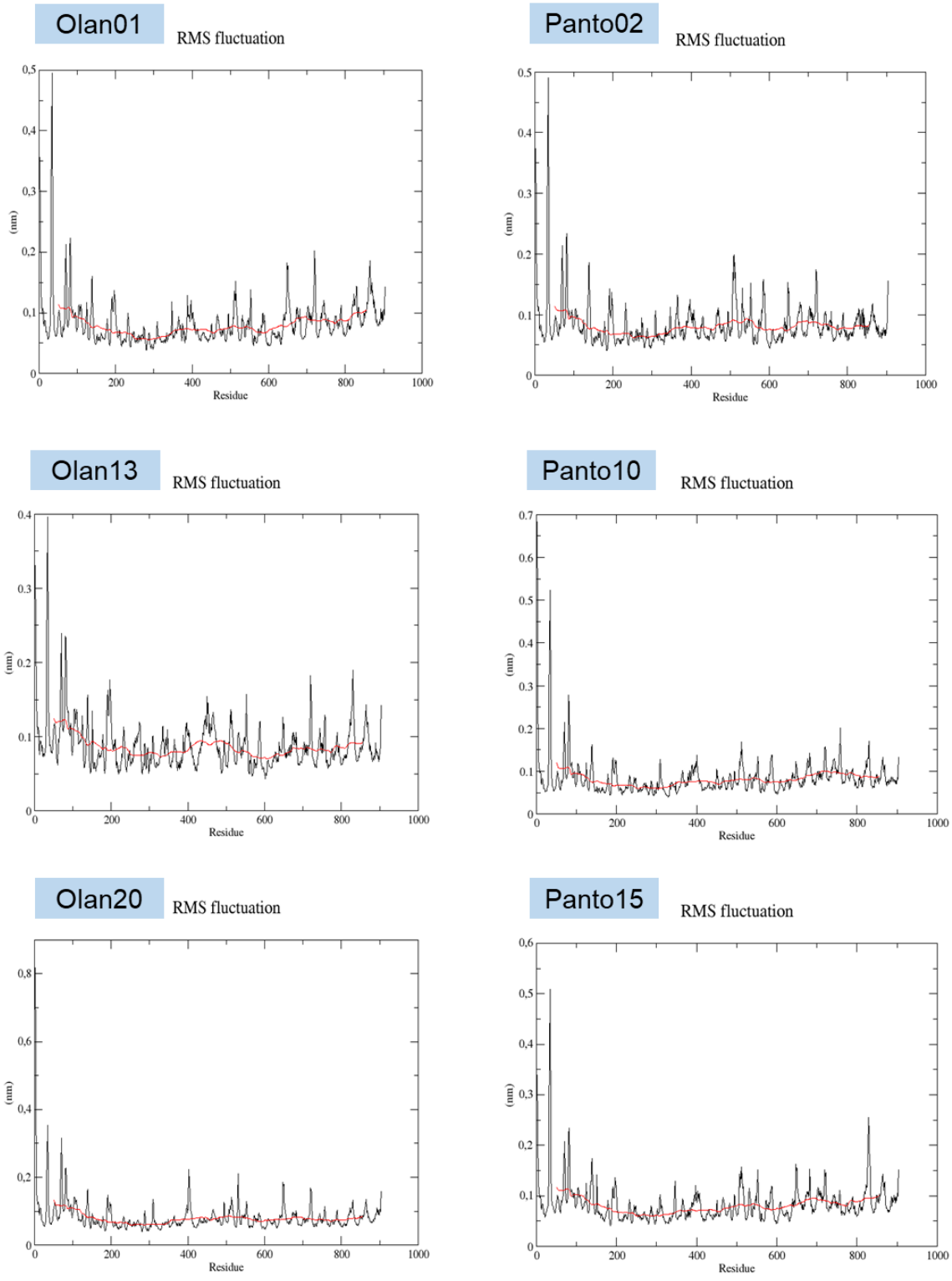

Figure 13. The root-mean-square fluctuation (RMSF) measures the average deviation of the protein over 50 ns time from the reference position.

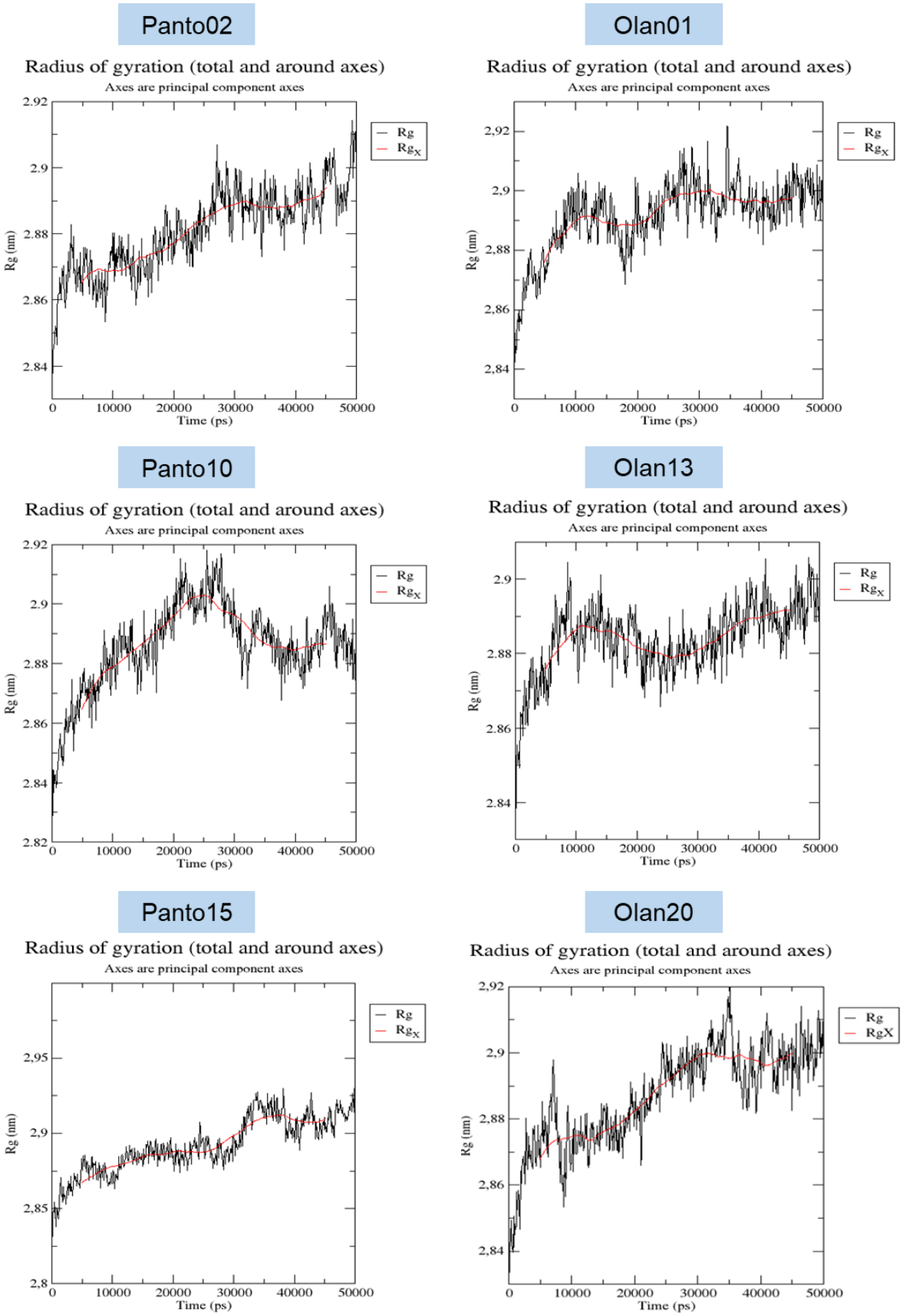

Figure 14. The radius of gyration (rGyr) graphs of the complexes for a total of 50ns.

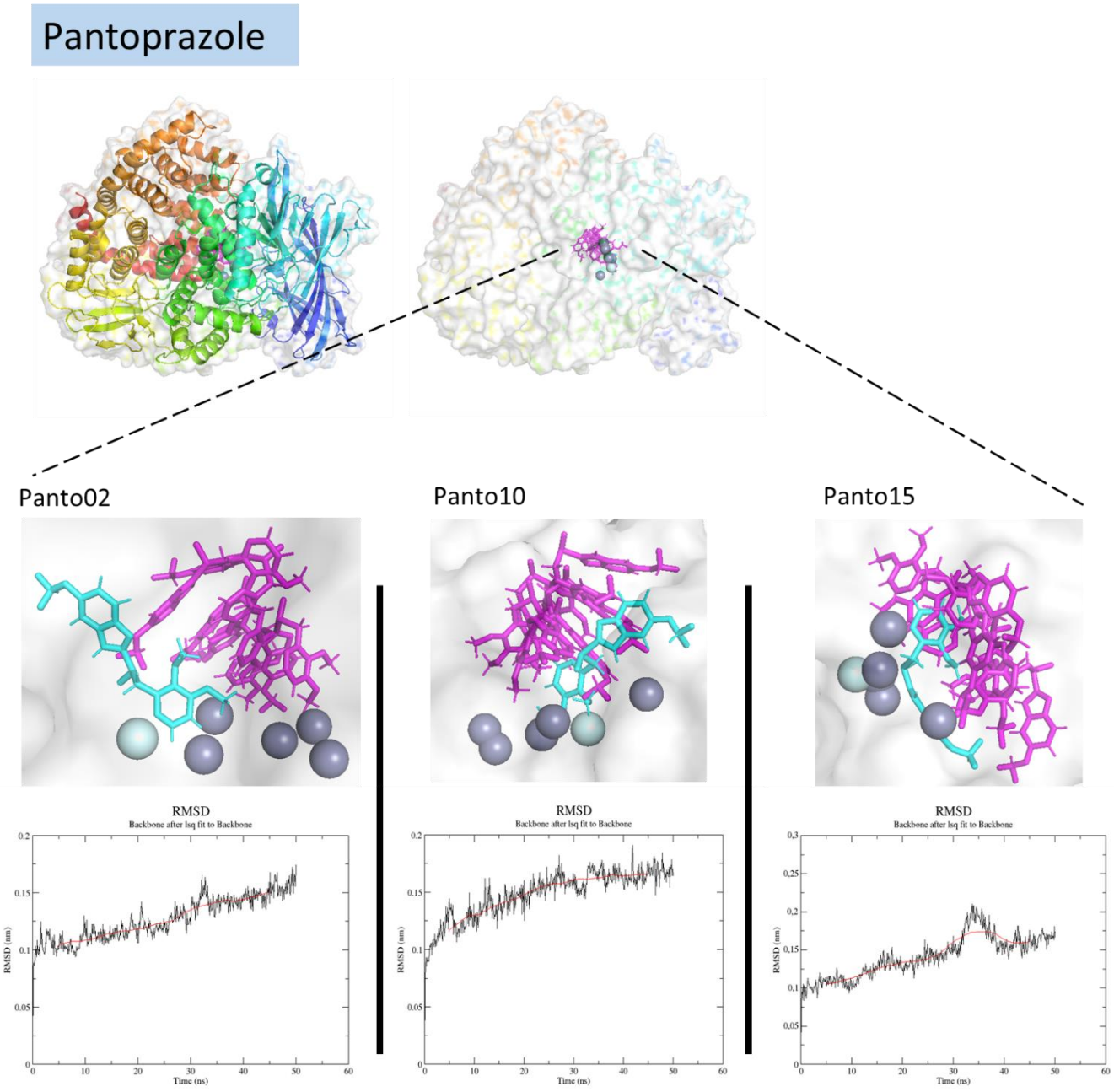

Figure 15. Shows the assessment of 50 ns MD simulation trajectories for the ANPEP-Pantoprazole complexes by superposing various orientation of ligand attained during MD simulation, and the Root-mean-square deviation (RMSD) graphs of atomic positions for a total of 50ns. The spheres represent the zinc ion.

Olanzapine

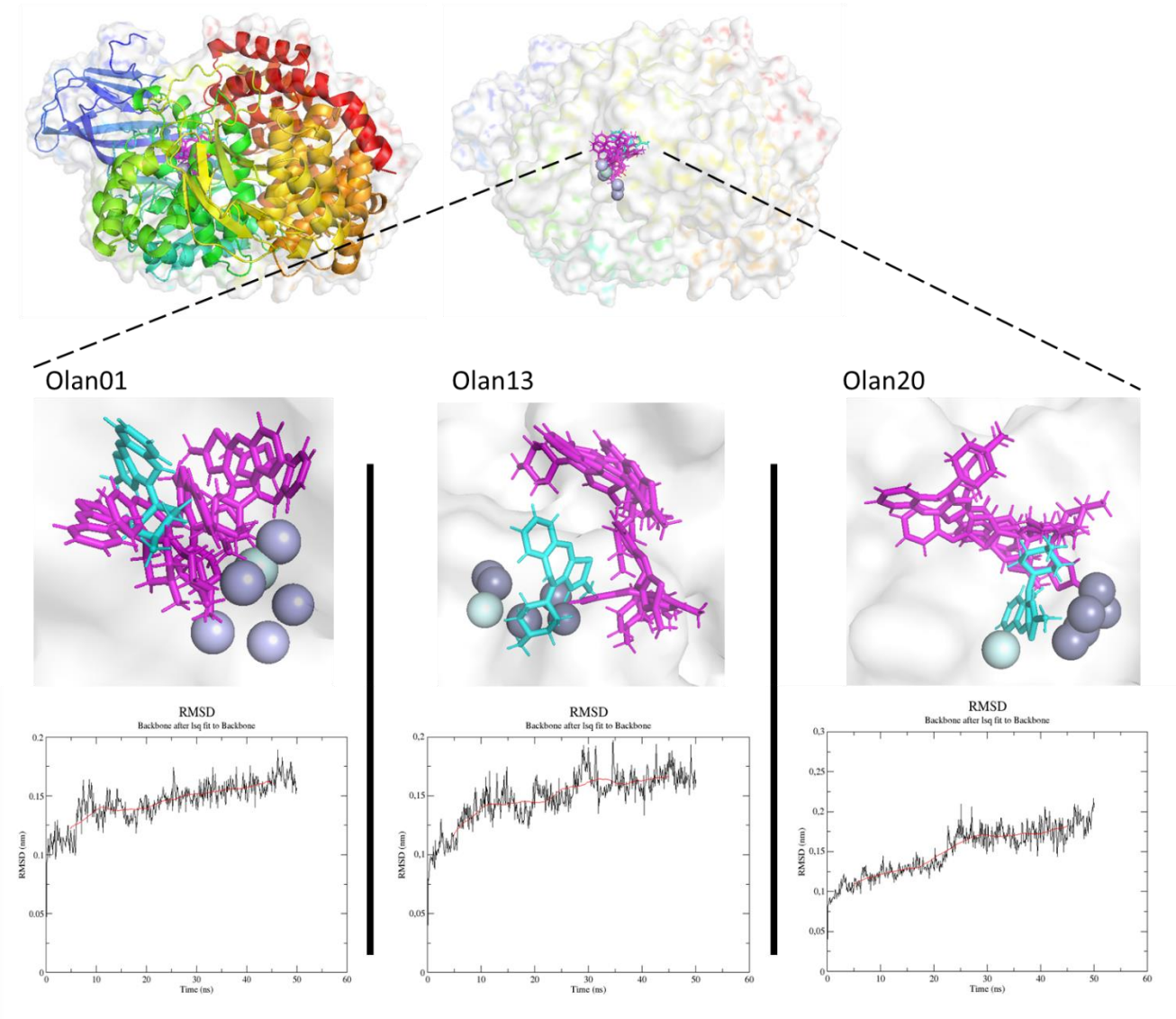

Figure 16. Shows the assessment of 50 ns MD simulation trajectories for the ANPEP-Olanzapine complexes by superposing various orientation of ligand attained during MD simulation, and the Root-mean-square deviation (RMSD) graphs of atomic positions for a total of 50ns. The spheres represent the zinc ion.

The MD simulation of the complexes was performed to evaluate their stability and interactions over time. The RMSD and RMSF are common measures of biomolecules' spatial variations in a MD simulation. RMSD describes the molecule's overall discrepancy with respect to a reference conformation, while RMSF measures the displacement of a particular atom or Molecular Diversity group of atoms relative to the reference structure.

The poses attained by the ligand at an interval of 10 ns timeframe of the 50 ns simulation for the docked complex of ANPEP-Pantoprazole are shown in **fig15**. **Fig16** shows the same for the docked complex of ANPEP-Olanzapine. The RMSD plots of all complexes showed that the protein and ligand structures were stable throughout the simulation, with values below 3 Å for the protein. The average RMSD values of olan1, olan13, panto2 panto10, panto15 and Bestatin complexes were lower than <2 Å suggesting that the complexes are stable (**fig15.**) (**fig16.**). It is important to highlight the need for longer simulations, as the poses of conformations from both Olanzapine and Pantoprazole show deviation from each other, in the binding pocket. The RMSF plots revealed that both ligands induced similar fluctuations in the protein backbone, with higher values observed for some residues in the active site (**fig13.**).

The radius of gyration (rGyr) is another parameter that reflects the compactness of a protein structure. The rGyr plots of both complexes showed that the protein–ligand systems maintained a similar degree of compactness throughout the simulation, indicating that no major conformational changes occurred upon ligand binding. These findings are consistent with the docking results, which showed that Olanzapine and Pantoprazole have similar binding modes and energies with ANPEP. The rGyr offers insights into the compactness of system's structure. It was found to be lower than 2.9 Å in ANPEP-Bestatin (**fig12.**). The other complexes have a slightly higher maximum rGyr around 2.92 Å, except panto15 which had the highest (**fig14.**), suggesting a broader distribution of the ligand within the active site of ANPEP and indicating potentially more effective engagement and interactions with the active site residues. These results suggest that both Olanzapine and Pantoprazole bind to ANPEP with comparable affinity and flexibility, and that they share some key interactions with the active site residues.

DISCUSSION

ERK pathway

The analysis of the upregulated genetic signature of claudin low showed that the most influential nodes were *TGFBR2, JUN* and *CD44*. These genes participate in a positive feedback loop between powered primarily by the activation of the ERK pathway whose downstream events favor the continuous expression of the genes. Furthermore, the gene ontology terms of the genes targeted by the suggested compound lists were analyzed, indicating that the “GABA alpha receptor activity” term is shared among all the results. The GABAAR possesses phosphorylation sites for ERK in its alpha subunits, indicating a possible association with the ERK pathway.

There is currently a lot of interest in finding ways to develop effective inhibitors for ERK1/2 as a potential therapy for various cancers. Since Raf and MEK inhibitors have been found to be successful and the MAP kinase pathway follows a linear pathway (Ras-Raf-MEK-ERK), it makes sense to target ERK, which is the terminal kinase of the pathway (Roskoski, 2019). Furthermore, cancers can become resistant to Raf and MEK inhibitors due to reactivation of the signaling module, making it necessary to target ERK as an additional approach to prevent acquired resistance and achieve a primary therapeutic response. Although ERK is a potential target for drug development, there has been slower progress in developing clinically effective inhibitors for it compared to Raf and MEK inhibitors (Roskoski, 2019). ERK has a highly conserved structure, making it difficult to directly target it specifically without affecting other kinases with similar structures (Roberts & Der, 2007; Roskoski, 2012). Finally, ERK is involved in a variety of cellular processes, including cell proliferation, differentiation, and survival, which makes it harder to target it without causing significant side effects (Roberts & Der, 2007; Roskoski, 2012).

Inhibition of the π-subunit of GABAAR represents an alternative approach to work around this problem to reduce Claudin-low development, reducing ERK’s activation without directly targeting it. Another approach showed that tumour invasiveness and proliferation of CNS and other systemic malignancies can be reduced by boosting GABAergic signaling by using GABAAR positive allosteric modulators such as benzodiazepines (Bhattacharya et al., 2021). Additionally, increased activation of GABAAR is shown to can make cancer cells more susceptible to radiation, chemotherapeutic agents, and immune checkpoint inhibitors (Bhattacharya et al., 2021). A brain-penetrant anxiolytic that is therapeutically available and has the potential to treat cancer should be a welcome addition to the anti-cancer toolbox. As obvious as it seems that phosphorylation affects GABAAR allosteric modulation, the molecular mechanisms governing these activities are currently unknown. Moreover, it is still unknown whether phosphorylation affects modulator-induced alterations to channel gating or whether it promotes the binding of allosteric modulators to receptors. However, undoubtedly phosphorylation adds more

variety to how GABAARs and allosteric modulators interact (Nakamura et al., 2015). Finally, the potential association of GABAAR with the development and progression of CLBC should be further investigated.

Drug categories

The CM and MCF7 compound lists from Connectivity Map analysis (**Supplementary Table1 & Table2**) include compounds able to reverse the upregulated gene expression pattern associated with the claudin-low subtype, while the compounds of the structurally determined list of Autodock Vina (**Supplementary Table1**) have the potential to interact and inhibit the ANPEP protein. With further analysis of the suggested compound lists, most compounds (>50%) were found to fall in one of the four general disease areas (psychiatric, infectious, endocrinology, and gastroenterology). These areas may provide a starting point to identify more compounds able to combat CL and determine relevant mechanisms of action.

Antipsychotic medications' great potential as neo-adjuvants and potential chemotherapeutics in single or multimodal treatment approaches is demonstrated by their capacity to modulate a variety of signaling pathways and multidrug resistance-conferring proteins that improve the efficacy of chemotherapeutic drugs with minimal side effects (Kamarudin & Parhar, 2019). Molecules that have been identified as GABAAR targets fall under the psychiatric category. For instance, benzodiazepines, like diazepam, have antiproliferative effects on breast cancer cells both in vitro and in vivo (Kamarudin & Parhar, 2019).

The infectious disease category includes molecules like antibiotics having anti-proliferative, anti-apoptotic, and anti-EMT effect. However, the resulting disturbance of intestine flora is a double-edged blade for the effective treatment of cancer. The area of endocrinology is an equally important category, since it employs hormones for the targeting of specific receptors of the autocrine system intercellular communication.

Finally, the gastroenterology area, that also includes Pantoprazole and other drugs with similar proton pump inhibitory action, are proposed in literature for repurposing in breast cancer, as they can offer drug sensitivity by altering the pH of the stomach (Wang et al., 2021). The stomach's acidic environment can impact the absorption and efficacy of certain medications (Wang et al., 2021). By reducing stomach acid production, PPIs can increase the bioavailability of some drugs, allowing for more efficient absorption and potentially enhancing their effectiveness. Drugs in these areas show most potential of showing an effect on CL subtype and its migratory capabilities.

Olanzapine and Pantoprazole

ANPEP participates in tumour cell motility and is overexpressed in many cancers including colorectal, pancreatic, and liver cancer (Mina-osorio, 2008). In addition, claudin-low breast cancer is mostly characterized by its migratory capabilities. Olanzapine and Pantoprazole are both found to bind/inhibit ANPEP, while also reversing the genetic signature of CL. This overlap suggests that these drugs could be relevant in reducing the migratory effect of claudin-low breast cancer.

Olanzapine, an atypical benzodiazepine, was found to have weak affinity with the GABAAR, but showed some contradictory expression effects, as it positively regulates SNCA, and might increase the activity of AP-1 complex, in neuroblastoma cells (Filatova et al., 2017) (Finch et al., 2002). However, benzodiazepines act as allosteric modulators to GABAARs, enhancing the effect of GABA (Bhattacharya et al., 2021) and eliciting a chloride efflux, able to induce apoptosis of cells in melanoma and medulloblastoma, by depolarizing their mitochondria (Bhattacharya et al., 2021). They mediate a significant regression in tumour size, even at a concentration equivalent to what an adult would take as an anxiolytic. Nevertheless, the effect of Olanzapine on the viability of TNBC cells hasn't been demonstrated yet, requiring more physiological experiments to test their response in Olanzapine treatment.

Pantoprazole has already been characterized as a potential candidate drug for TNBC, without referring to any association with GABAAR. Even though PPZ is not a benzodiazepine compound, docking analysis should be conducted to determine any allosteric modulatory capabilities in GABAAR. Feng et al. (2016) proposed that the use of PPZ treatment shows potential in fighting against CSCs and preventing tumour recurrence. Moreover, research conducted by Andang et al. (2008) demonstrated that GABAAR signaling induces the accumulation of stem cells in the S phase, resulting in a significant decrease in cell proliferation. However, the broader implications of GABA and GABAAR in cellular signaling outside of synapses have not been extensively explored. Therefore, it is crucial to further investigate the mechanisms through which PPZ affects CSCs and determine potential direct or indirect connections with GABAAR signaling. Such investigations would contribute to the development of more efficient therapies targeting these cells.

CONCLUSION

The suggested molecules, Pantoprazole, and Olanzapine may be candidate repurposed drugs. However, it is important to note that structural interaction alone does not guarantee therapeutic efficacy, and further experimental validation is required to confirm the effectiveness of the identified drugs. Conducting in vitro experiments on cancer cells derived from the claudin-low subtype can help confirm the potential effectiveness of the prioritized drugs in targeting the specific upregulated genes. Overall, the drug lists and the disease-area summary provide complementary information that can help guide further experimental investigation into potential therapeutic candidates for the CL subtype.

REFERENCES

Andäng, M., Hjerling-Leffler, J., Moliner, A., Lundgren, T. K., Castelo-Branco, G., Nanou, E., Pozas, E., Bryja, V., Halliez, S., Nishimaru, H., Wilbertz, J., Arenas, E., Koltzenburg, M., Charnay, P., El Manira, A., Ibañez, C. F., & Ernfors, P. (2008). Histone H2AX-dependent GABA(A) receptor regulation of stem cell proliferation. Nature, 451(7177), 460–464. https://doi.org/10.1038/nature06488

Angel, P., Hattori, K., Smeal, T., & Karin, M. (1988). The jun proto-oncogene is positively autoregulated by its product, Jun/AP-1. *Cell*, *55*(5), 875–885. https://doi.org/10.1016/0092-8674(88)90143-2

Banerjee, S., Modi, S., McGinn, O., Zhao, X., Dudeja, V., Ramakrishnan, S., & Saluja, A. K. (2016). Impaired Synthesis of Stromal Components in Response to Minnelide Improves Vascular Function, Drug Delivery, and Survival in Pancreatic Cancer. *Clinical cancer research : an official journal of the American Association for Cancer Research*, *22*(2), 415–425. https://doi.org/10.1158/1078-0432.CCR-15-1155

Beberok, A., Wrześniok, D., Rok, J., Rzepka, Z., Respondek, M., & Buszman, E. (2018). Ciprofloxacin triggers the apoptosis of human triple-negative breast cancer MDA-MB-231 cells via the p53/Bax/Bcl-2 signaling pathway. *International journal of oncology*, *52*(5), 1727–1737. https://doi.org/10.3892/ijo.2018.4310

Bell-Horner, C. L., Dohi, A., Nguyen, Q., Dillon, G. H., & Singh, M. (2006). ERK/MAPK pathway regulates GABAA receptors. *Journal of neurobiology*, *66*(13), 1467–1474. https://doi.org/10.1002/neu.20327

Bhatt, A. B., Patel, S., Matossian, M. D., Ucar, D. A., Miele, L., Burow, M. E., Flaherty, P. T., & Cavanaugh, J. E. (2021). Molecular Mechanisms of Epithelial to Mesenchymal Transition Regulated by ERK5 Signaling. *Biomolecules*, *11*(2), 183. https://doi.org/10.3390/biom11020183

Bhattacharya, D., Gawali, V. S., Kallay, L., Toukam, D. K., Koehler, A., Stambrook, P., Krummel, D. P., & Sengupta, S. (2021). Therapeutically leveraging $GABA_A$ receptors in cancer. *Experimental biology and medicine (Maywood, N.J.)*, *246*(19), 2128–2135. https://doi.org/10.1177/15353702211032549

Brady, M. L., Pilli, J., Lorenz-Guertin, J. M., Das, S., Moon, C. E., Graff, N., & Jacob, T. C. (2018). Depolarizing, inhibitory GABA type A receptor activity regulates GABAergic synapse plasticity via ERK and BDNF signaling. *Neuropharmacology*, *128*, 324–339. https://doi.org/10.1016/j.neuropharm.2017.10.022

Brennan, A., Leech, J. T., Kad, N. M., & Mason, J. M. (2020). Selective antagonism of cJun for cancer therapy. *Journal of experimental & clinical cancer research : CR*, *39*(1), 184. https://doi.org/10.1186/s13046-020-01686-9

Buonato, J. M., & Lazzara, M. J. (2014). ERK1/2 blockade prevents epithelial-mesenchymal transition in lung cancer cells and promotes their sensitivity to EGFR inhibition. Cancer research, 74(1), 309–319. https://doi.org/10.1158/0008-5472.CAN-12-4721.

Calaf, G. M., Crispin, L. A., Muñoz, J. P., Aguayo, F., & Bleak, T. C. (2022). Muscarinic Receptors Associated with Cancer. *Cancers*, *14*(9), 2322. https://doi.org/10.3390/cancers14092322

Carl-McGrath, S., Ebert, M. P., Lendeckel, U., & Malfertheiner, P. (2004). The role of aminopeptidase N/CD13 in gastrointestinal cancer. Digestive Diseases and Sciences, 49(5), 902-906.

Cha, Y., Erez, T., Reynolds, I. J., Kumar, D., Ross, J., Koytiger, G., Kusko, R., Zeskind, B., Risso, S., Kagan, E., Papapetropoulos, S., Grossman, I., & Laifenfeld, D. (2018). Drug repurposing from the perspective of pharmaceutical companies. *British journal of pharmacology*, *175*(2), 168–180. https://doi.org/10.1111/bph.13798

Challener, C. A. (2018). Can artificial intelligence take the next step for drug repositioning. *Pharma Technol*, *42*(9), 22-25.

Chen, C., Zhao, S., Karnad, A. et al. The biology and role of CD44 in cancer progression: therapeutic implications. *J Hematol Oncol* **11**, 64 (2018). https://doi.org/10.1186/s13045-018-0605-5

Chen, L. & Bourguignon, L.Y.W. (2014) Hyaluronan-CD44 interaction promotes c-Jun signaling and miRNA21 expression leading to Bcl-2 expression and chemoresistance in breast cancer cells. *Mol Cancer* **13**, 52. https://doi.org/10.1186/1476-4598-13-52

Chen, L., Lin, Y. L., Peng, G., & Li, F. (2012). Structural basis for multifunctional roles of mammalian aminopeptidase N. Proceedings of the National Academy of Sciences, 109(45), 17966-17971.

Chen, L., Lin, Y.-L., Peng, G., & Li, F. (2012). Structural basis for multifunctional roles of mammalian aminopeptidase N. Proceedings of the National Academy of Sciences, 109(44), 17966-17971. doi: 10.1073/pnas.1210123109

Chesbrough, H., & Chen, E. L. (2013). Recovering abandoned compounds through expanded external IP licensing. *California Management Review*, *55*(4), 83-101.

Cortez M, Langreth R. Biogen resumes Alzheimer's studies to offer controversial drug. Bloomberg News. Bloomberg. 2019. Cited 20 Aug 2021. Available from: https://www.bnnbloomberg.ca/biogen-resumes-alzheimer-s-studies-to-offer-controversial-drug-1.1358152.

Danziger, R. S. (2008). Aminopeptidase N in arterial hypertension. Heart Failure Reviews, 13(3), 293-298.

Datar, P., Srivastava, S., Coutinho, E., & Govil, G. (2004). Substance P: Structure, function, and therapeutics. Current Topics in Medicinal Chemistry, 4(1), 75-103.

Eberhardt, J., Santos-Martins, D., Tillack, A.F., Forli, S. (2021). AutoDock Vina 1.2.0: New Docking Methods, Expanded Force Field, and Python Bindings. Journal of Chemical Information and Modeling.

Feng, S., Zheng, Z., Feng, L., Yang, L., Chen, Z., Lin, Y., Gao, Y., & Chen, Y. (2016). Proton pump inhibitor Pantoprazole inhibits the proliferation, self-renewal and chemoresistance of gastric cancer stem cells via the EMT/β-catenin pathways. *Oncology reports*, *36*(6), 3207–3214. https://doi.org/10.3892/or.2016.5154

Filatova, E., Kasian, A., Kolomin, T., Rybalkina, E., Alieva, A., Andreeva, L., Limborska, S., Myasoedov, N., Pavlova, G., Slominsky, P., & Shadrina, M. (2017). GABA, Selank, and Olanzapine Affect the Expression of Genes Involved in GABAergic Neurotransmission in IMR-32 Cells. *Frontiers in pharmacology*, *8*, 89. https://doi.org/10.3389/fphar.2017.00089

Finch, S., Joseloff, E., & Bowden, T. (2002). JunB negatively regulates AP-1 activity and cell proliferation of malignant mouse keratinocytes. *Journal of cancer research and clinical oncology*, *128*(1), 3–10. https://doi.org/10.1007/s00432-001-0298-x

Follesa, P., Porcu, P., Sogliano, C., Cinus, M., Biggio, F., Mancuso, L., Mostallino, M.C., Paoletti, A.M., Purdy, R.H., Biggio, G., and Concas, A. (2005). Changes in GABA(A) receptor gene expression induced by withdrawal of, but not by long-term treatment with, benzodiazepine full or partial agonists. Brain Res. Mol. Brain Res. 135, 124-132

Fougner, C., Bergholtz, H., Norum, J. H., & Sørlie, T. (2020). Re-definition of claudin-low as a breast cancer phenotype. Nat Commun 11, 1787. https://doi.org/10.1038/s41467-020-15574-5.

Frail, D. E., Brady, M., Escott, K. J., Holt, A., Sanganee, H. J., Pangalos, M. N., Watkins, C., & Wegner, C. D. (2015). Pioneering government-sponsored drug repositioning collaborations: progress and learning. *Nature reviews. Drug discovery*, *14*(12), 833–841. https://doi.org/10.1038/nrd4707

Gao, Y., Shang, Q., Li, W., Guo, W., Stojadinovic, A., Mannion, C., Man, Y. G., & Chen, T. (2020). Antibiotics for cancer treatment: A double-edged sword. *Journal of Cancer*, *11*(17), 5135–5149. https://doi.org/10.7150/jca.47470

Gee, J. M., Barroso, A. F., Ellis, I. O., Robertson, J. F., & Nicholson, R. I. (2000). Biological and clinical associations of c-jun activation in human breast cancer. *International journal of cancer*, *89*(2), 177–186. https://doi.org/10.1002/(sici)1097-0215(20000320)89:2<177:aid-ijc13>3.0.co;2-0

Goh, W., Sleptsova-Freidrich, I., & Petrovic, N. (2014). Use of proton pump inhibitors as adjunct treatment for triple-negative breast cancers. An introductory study. *Journal of pharmacy & pharmaceutical sciences: a publication of the Canadian Society for Pharmaceutical Sciences, Societe canadienne des sciences pharmaceutiques*, *17*(3), 439–446. https://doi.org/10.18433/j34608

Graul, A. I., Sorbera, L., Pina, P., Tell, M., Cruces, E., Rosa, E., Stringer, M., Castañer, R., & Revel, L. (2010). The Year's New Drugs & Biologics - 2009. *Drug news & perspectives*, *23*(1), 7–36. https://doi.org/10.1358/dnp.2010.23.1.1440373

Guo W, Keckesova Z, Donaher JL, Shibue T, Tischler V, Reinhardt F, et al. (2012). Slug and Sox9 cooperatively determine the mammary stem cell state. Cell, 148(5): 1015-1028.

Gupta, P. B., Onder, T. T., Jiang, G., Tao, K., Kuperwasser, C., Weinberg, R. A., & Lander, E. S. (2009). Identification of selective inhibitors of cancer stem cells by high-throughput screening. Cell, 138(4), 645â659. https://doi.org/10.1016/j.cell.2009.06.034

Hao, Y., Baker, D., & Ten Dijke, P. (2019). TGF-β-Mediated Epithelial-Mesenchymal Transition and Cancer Metastasis. *International journal of molecular sciences*, *20*(11), 2767. https://doi.org/10.3390/ijms20112767

Hashida, H., Takabayashi, A., Kanai, M., Adachi, M., Kondo, K., Kohno, N., & Yamaoka, Y. (2002). Aminopeptidase N is involved in cell motility and angiogenesis: its clinical significance in human colon cancer. Gastroenterology, 122(2), 376-386.

Hauser, A. S., Attwood, M. M., Rask-Andersen, M., Schiöth, H. B., & Gloriam, D. E. (2017). Trends in GPCR drug discovery: new agents, targets and indications. *Nature reviews. Drug discovery*, *16*(12), 829–842. https://doi.org/10.1038/nrd.2017.178

Huang, daW., Sherman, B. T., & Lempicki, R. A. (2009). Systematic and integrative analysis of large gene lists using DAVID bioinformatics resources. *Nature protocols*, *4*(1), 44–57. https://doi.org/10.1038/nprot.2008.211

Iacopetta, D., Rechoum, Y., & Fuqua, S. A. (2012). The Role of Androgen Receptor in Breast Cancer. *Drug discovery today. Disease mechanisms*, *9*(1-2), e19–e27. https://doi.org/10.1016/j.ddmec.2012.11.003

Ihraiz, W. G., Ahram, M., & Bardaweel, S. K. (2020). Proton pump inhibitors enhance chemosensitivity, promote apoptosis, and suppress migration of breast cancer cells. *Acta pharmaceutica (Zagreb, Croatia)*, *70*(2), 179–190. https://doi.org/10.2478/acph-2020-0020

In, W., Lu, Z., Li, Q., Wang, Q., Wang, J., Zhang, Y., Qian, H., Chen, Y., Chen, X., & Chen, L. (2014). GABA-A receptor regulates ERK1/2 activation in breast cancer cells. PLoS One, 9(5), e97923. doi: 10.1371/journal.pone.0097923. PMID: 24857983.

Ishii, K., Usui, S., Yamamoto, H., Sugimura, Y., Yokoo, S., Iriyama, C., & Tamaoki, T. (2001). Aminopeptidase N regulated by zinc in human prostate participates in tumor cell invasion. International Journal of Cancer, 92(1), 49-54.

Jiang WG, Watkins G, Douglas-Jones A, et al. Prostaglandin synthase 2/cyclooxygenase 2 (COX2) and COX2-associated protein expression in human breast cancer. Anticancer Res. 2006;26(6B):4297-301. PMID: 17201145.

Jing Y, Xia L, Lu Y, Wu Y, Wang A, Wang J, Yang Y, Nie Y, Fan D. Expression of PTGS2 and PPARγ in human gastric cancer: a correlation with clinical pathological parameters. PLoS One. 2014 Jul 10;9(7):e101251. doi: 10.1371/journal.pone.0101251.

Jonas, O., Calligaris, D., Methuku, K. R., Poe, M. M., Francois, J. P., Tranghese, F., Changelian, A., Sieghart, W., Ernst, M., Krummel, D. A., Cook, J. M., Pomeroy, S. L., Cima, M., Agar, N. Y., Langer, R., & Sengupta, S. (2016). First In Vivo Testing of Compounds Targeting Group 3 Medulloblastomas Using an Implantable Microdevice as a New Paradigm for Drug Development. *Journal of biomedical nanotechnology*, *12*(6), 1297–1302. https://doi.org/10.1166/jbn.2016.2262

Joo, M. K., Park, J. J., & Chun, H. J. (2019). Proton pump inhibitor: The dual role in gastric cancer. *World journal of gastroenterology*, *25*(17), 2058–2070. https://doi.org/10.3748/wjg.v25.i17.2058

Jordan, V. C. (2003). Tamoxifen: a most unlikely pioneering medicine. Nature Reviews Cancer, 3(6), 1-9. doi:10.1038/nrc1073

Judd, N. P., Winkler, A. E., Murillo-Sauca, O., Brotman, J. J., Law, J. H., Lewis, J. S., Jr, Dunn, G. P., Bui, J. D., Sunwoo, J. B., & Uppaluri, R. (2012). ERK1/2 regulation of CD44 modulates oral cancer aggressiveness. *Cancer research*, *72*(1), 365–374. https://doi.org/10.1158/0008-5472.CAN-11-1831

Kallay, L., Keskin, H., Ross, A., Rupji, M., Moody, O. A., Wang, X., Li, G., Ahmed, T., Rashid, F., Stephen, M. R., Cottrill, K. A., Nuckols, T. A., Xu, M., Martinson, D. E., Tranghese, F., Pei, Y., Cook, J. M., Kowalski, J., Taylor, M. D., Jenkins, A., … Sengupta, S. (2019). Modulating native $GABA_A$ receptors in medulloblastoma with positive allosteric benzodiazepine-derivatives induces cell death. *Journal of neuro-oncology*, *142*(3), 411–422. https://doi.org/10.1007/s11060-019-03115-

Kamarudin M. N.A., Parhar I. Emerging therapeutic potential of anti-psychotic drugs in the management of human glioma: A comprehensive review. Oncotarget. 2019; 10: 3952-3977. Retrieved from https://www.oncotarget.com/article/26994/text/

Katare, P. B., & Banerjee, S. K. (2016). Repositioning of Drugs in Cardiometabolic Disorders: Importance and Current Scenario. *Current topics in medicinal chemistry*, *16*(19), 2189–2200. https://doi.org/10.2174/1568026616666160216152138

Kayahara, M., Wang, X., & Tournier, C. (2005). Selective regulation of c-jun gene expression by mitogen-activated protein kinases via the 12-o-tetradecanoylphorbol-13-acetate- responsive element and myocyte enhancer factor 2 binding sites. *Molecular and cellular biology*, *25*(9), 3784–3792. https://doi.org/10.1128/MCB.25.9.3784-3792.2005

Kleinerman, R. A., Brinton, L. A., Hoover, R., & Fraumeni, J. F., Jr (1984). Diazepam use and progression of breast cancer. Cancer research, 44(3), 1223â1225.

König, M., Zimmer, A. M., Steiner, H., Holmes, P. V., Crawley, J. N., Brownstein, M. J., ... & Zimmer, A. (1996). Pain responses, anxiety and aggression in mice deficient in pre-proenkephalin. Nature, 383(6600), 535-538.

Krishnamurthy, N., Grimshaw, A.A., Axson, S.A. et al. Drug repurposing: a systematic review on root causes, barriers and facilitators. *BMC Health Serv Res* 22, 970 (2022). https://doi.org/10.1186/s12913-022-08272-z

Lamb, R. F., Hennigan, R. F., Turnbull, K., Katsanakis, K. D., MacKenzie, E. D., Birnie, G. D., & Ozanne, B. W. (1997). AP-1-mediated invasion requires increased expression of the hyaluronan receptor CD44. *Molecular and cellular biology*, *17*(2), 963–976. https://doi.org/10.1128/MCB.17.2.963

Lee, A. V., Oesterreich, S., & Davidson, N. E. (2015). MCF-7 cells--changing the course of breast cancer research and care for 45 years. *Journal of the National Cancer Institute*, *107*(7), djv073. https://doi.org/10.1093/jnci/djv073

Lee, M. K., Pardoux, C., Hall, M. C., Lee, P. S., Warburton, D., Qing, J., Smith, S. M., & Derynck, R. (2007). TGF-beta activates Erk MAP kinase signalling through direct phosphorylation of ShcA. *The EMBO journal*, *26*(17), 3957–3967. https://doi.org/10.1038/sj.emboj.7601818

Lehmann, B. D., Bauer, J. A., Chen, X., Sanders, M. E., Chakravarthy, A. B., Shyr, Y., & Pietenpol, J. A. (2011). Identification of human triple-negative breast cancer subtypes and preclinical models for selection of targeted therapies. Journal of Clinical Investigation, 121(7), 2750-2767.

Leonzino, M., Busnelli, M., Antonucci, F., Verderio, C., Mazzanti, M., & Chini, B. (2016). The Timing of the Excitatory-to-Inhibitory GABA Switch Is Regulated by the Oxytocin Receptor via KCC2. *Cell reports*, *15*(1), 96–103. https://doi.org/10.1016/j.celrep.2016.03.013

Lichner, Z., Saleh, C., Subramaniam, V., Seivwright, A., Prud'homme, G. J., & Yousef, G. M. (2015). miR-17 inhibition enhances the formation of kidney cancer spheres with stem cell/ tumor initiating cell properties. Oncotarget, 6(8), 5567â5581. https://doi.org/10.18632/oncotarget.1901

Liu H, Zang C, Emde A, Planas-Silva MD, Rosche M, Kühnl A, et al. (2006) Global gene expression profiles of human head and neck squamous carcinoma cell lines. Int J Cancer 118: 1932–1941. doi: 10.1002/ijc.21599.

Lizaur-Utrilla, A., Collados-Maestre, I., Miralles-Muñoz, F. A., & Lopez-Prats, F. A. (2015). Total Knee Arthroplasty for Osteoarthritis Secondary to Fracture of the Tibial Plateau. A Prospective Matched Cohort Study. The Journal of arthroplasty, 30(8), 1328–1332. https://doi.org/10.1016/j.arth.2015.02.032

López-Cortés, G.I.; Palacios-Pérez, M.; Hernández-Aguilar, M.M.; Veledíaz, H.F.; José, M.V. (2023). Human Coronavirus Cell Receptors Provide Challenging Therapeutic Targets. Vaccines, 11, 174. https://doi.org/10.3390/vaccines11010174.

Lowes, H., Pyle, A., Duddy, M., & Parkinson, M. H. (2020). The human coronavirus receptor ANPEP (CD13) is overexpressed in Parkinson's disease. Movement Disorders, 35(12), 2324-2325.

Lu, C., Amin, M. A., & Fox, D. A. (2020). CD13/aminopeptidase N is a potential therapeutic target for inflammatory disorders. The Journal of Immunology, 204(1 Supplement), 3-11.

Luo K. (2017). Signaling Cross Talk between TGF-β/Smad and Other Signaling Pathways. *Cold Spring Harbor perspectives in biology*, *9*(1), a022137.

Manzetti, S., Xu, X., Barone, V., & Hallberg, A. (2003). 3D-QSAR and pharmacophore modeling of aminopeptidase N inhibitors. Journal of Medicinal Chemistry, 46(7), 981-992. doi: 10.1021/jm020904g

Marcath, L.A.; Coe, T.D.; Hoylman, E.K.; Redman, B.G.; Hertz, D.L. Prevalence of drug-drug interactions in oncology patients enrolled on National Clinical Trials Network oncology clinical trials. BMC Cancer, 2018, 18(1), 1155.

McCormick, C. A., Samuels, T. L., Battle, M. A., Frolkis, T., Blumin, J. H., Bock, J. M., Wells, C., Yan, K., Altman, K. W., & Johnston, N. (2021). H+/K+ATPase Expression in the Larynx of Laryngopharyngeal Reflux and Laryngeal Cancer Patients. *The Laryngoscope*, *131*(1), 130–135. https://doi.org/10.1002/lary.28643

Mestres, J., Gregori-Puigjané, E., Valverde, S., Solé, R. V., & Oliva, B. (2008). Data completeness—the Achilles heel of drug-target networks. Nature Biotechnology, 26(9), 983-984. doi: 10.1038/nbt0908-983

Midgley, A. C., Rogers, M., Hallett, M. B., Clayton, A., Bowen, T., Phillips, A. O., & Steadman, R. (2013). Transforming growth factor-β1 (TGF-β1)-stimulated fibroblast to myofibroblast differentiation is mediated by hyaluronan (HA)-facilitated epidermal growth factor receptor (EGFR) and CD44 co-localization in lipid rafts. *The Journal of biological chemistry*, *288*(21), 14824–14838. https://doi.org/10.1074/jbc.M113.451336

Mina-Osorio P. (2008). The moonlighting enzyme CD13: old and new functions to target. *Trends in molecular medicine*, *14*(8), 361–371. https://doi.org/10.1016/j.molmed.2008.06.003

Nachun, D., Gao, F., Isaacs, C., Guo, Y., Ray, K., Hasso, A. N., & Baloh, R. H. (2018). Peripheral blood gene expression reveals an inflammatory transcriptomic signature in Friedreich's ataxia patients. Human Molecular Genetics, 27(16), 2965-2977.

Nakamura, Y., Darnieder, L. M., Deeb, T. Z., & Moss, S. J. (2015). Regulation of GABAARs by phosphorylation. *Advances in pharmacology (San Diego, Calif.)*, *72*, 97–146. https://doi.org/10.1016/bs.apha.2014.11.008

Nam, K., Oh, S., Lee, K. M., Yoo, S. A., & Shin, I. (2015). CD44 regulates cell proliferation, migration, and invasion via modulation of c-Src transcription in human breast cancer cells. Cellular signalling, 27(9), 1882–1894. https://doi.org/10.1016/j.cellsig.2015.05.002

Naylor S, Schonfeld M. Therapeutic Drug Repurposing, Repositioning and Rescue Part I: Overview. Drug Discovery World. 2014. Cited 20 Aug 2021. Available from: https://www.ddw-online.com/therapeutic-drug-repurposing-repositioning-and-rescue-part-i-overview-1463-201412/.

Niraula, S., Dowling, R. J. O., Ennis, M., Chang, M. C., Done, S. J., Hood, N., ... & Pollak, M. (2012). Metformin in early breast cancer: a prospective window of opportunity neoadjuvant study. Breast Cancer Research and Treatment, 135(3), 821-830. doi: 10.1007/s10549-012-2204-1

Novack G. D. (2021). Repurposing medications. *The ocular surface*, *19*, 336–340. https://doi.org/10.1016/j.jtos.2020.11.012

Novoszel, P., Drobits, B., Holcmann, M. et al. The AP-1 transcription factors c-Jun and JunB are essential for CD8α conventional dendritic cell identity. *Cell Death Differ* **28**, 2404–2420 (2021). https://doi.org/10.1038/s41418-021-00765-4

Orian-Rousseau, V., & Ponta, H. (2008). Perspectives of CD44 targeting therapies. Archives of toxicology, 82(4), 211-213. doi: 10.1007/s00204-008-0295-4

Pantziarka, P.; Bouche, G.; André, N. "Hard" drug repurposing for precision oncology: The missing link? Front. Pharmacol., 2018, 9, 637. DOI: http://dx.doi.org/10.3389/fphar.2018.00637 PMID: 29962954

Papa, S., Choy, P. M., & Bubici, C. (2019). The ERK and JNK pathways in the regulation of metabolic reprogramming. *Oncogene*, *38*(13), 2223–2240. https://doi.org/10.1038/s41388-018-0582-8

Papamichail, A. (2023) Computational study of interaction networks between coding and non-coding rna molecules in claudin-low breast cancer subtype (Thesis).

Pommier, R. M., Sanlaville, A., Tonon, L., Kielbassa, J., Thomas, E., Ferrari, A., Sertier, A. S., Hollande, F., Martinez, P., Tissier, A., Morel, A. P., Ouzounova, M., & Puisieux, A. (2020). Comprehensive characterization of claudin-low breast tumors reflects the impact of the cell-of-origin on cancer evolution. *Nature communications*, *11*(1), 3431. https://doi.org/10.1038/s41467-020-17249-7

Prat, A., Parker, J. S., Karginova, O., Fan, C., Livasy, C., Herschkowitz, J. I., He, X., & Perou, C. M. (2010). Phenotypic and molecular characterization of the claudin-low intrinsic subtype of breast cancer. Breast Cancer Research, 12(5), R68.

Principe, D. R., Diaz, A. M., Torres, C., Mangan, R. J., DeCant, B., McKinney, R., Tsao, M. S., Lowy, A., Munshi, H. G., Jung, B., & Grippo, P. J. (2017). TGFβ engages MEK/ERK to differentially regulate benign and malignant pancreas cell function. *Oncogene*, *36*(30), 4336–4348. https://doi.org/10.1038/onc.2016.500

Principe, D. R., Doll, J. A., Bauer, J., Jung, B., Munshi, H. G., Bartholin, L., Pasche, B., Lee, C., & Grippo, P. J. (2014). TGF-β: duality of function between tumor prevention and carcinogenesis. *Journal of the National Cancer Institute*, *106*(2), djt369. https://doi.org/10.1093/jnci/djt369.

Pulley, J. M., Jerome, R. N., Shirey-Rice, J. K., Zaleski, N. M., Naylor, H. M., Pruijssers, A. J., Jackson, J. C., Bernard, G. R., & Holroyd, K. J. (2018). Advocating for mutually

beneficial access to shelved compounds. *Future medicinal chemistry*, *10*(12), 1395–1398. https://doi.org/10.4155/fmc-2018-0090

Pushpakom, S., Iorio, F., Eyers, P. A., Escott, K. J., Hopper, S., Wells, A., ... & Stathias, V. (2019). Drug repurposing: progress, challenges and recommendations. Nature Reviews Drug Discovery, 18(1), 41-58. doi: 10.1038/nrd.2018.168

Qu, Q., Tang, X., Kuang, B., Li, S., & Tu, G. (2015). 3D-QSAR Studies, Molecular Dynamics Simulation and Free Energy Calculation of APN Inhibitors. International Journal of Pharmacology, 11(8), 920-928. doi: 10.3923/ijp.2015.920.928

Rädler, P. D., Wehde, B. L., Triplett, A. A., Shrestha, H., Shepherd, J. H., Pfefferle, A. D., Rui, H., Cardiff, R. D., Perou, C. M., & Wagner, K. U. (2021). Highly metastatic claudin-low mammary cancers can originate from luminal epithelial cells. *Nature communications*, *12*(1), 3742. https://doi.org/10.1038/s41467-021-23957-5

Roberts, P. J., & Der, C. J. (2007). Targeting the Raf-MEK-ERK mitogen-activated protein kinase cascade for the treatment of cancer. Oncogene, 26(22), 3291-3310. https://doi.org/10.1038/sj.onc.1210422

Roskoski, R. Jr. (2012). ERK1/2 MAP kinases: structure, function, and regulation. Pharmacological research, 66(2), 105-143

Roskoski, R. Jr. (2019). Targeting ERK1/2 protein-serine/threonine kinases in human cancers. Pharmacological Research, 142, 151-168. doi: 10.1016/j.phrs.2019.03.009

Sánchez-Tilló, E., Fanlo, L., Siles, L., Montes-Moreno, S., Moros, A., Chiva-Blanch, G., Estruch, R., Martinez, A., Colomer, D., Győrffy, B., Roué, G., & Postigo, A. (2014). The EMT activator ZEB1 promotes tumor growth and determines differential response to chemotherapy in mantle cell lymphoma. *Cell death and differentiation*, *21*(2), 247–257. https://doi.org/10.1038/cdd.2013.123

Shahreza M, Ghadiri N, Mousavi SR, Varshosaz J, Green JR. A review of network-based approaches to drug repositioning. Brief Bioinform. 2018;19(5):878–92.

Shannon, P., Markiel, A., Ozier, O., Baliga, N. S., Wang, J. T., Ramage, D., Amin, N., Schwikowski, B., & Ideker, T. (2003). Cytoscape: a software environment for integrated models of biomolecular interaction networks. Genome research, 13(11), 2498–2504. https://doi.org/10.1101/gr.1239303

Sizemore, G. M., Sizemore, S. T., Seachrist, D. D., & Keri, R. A. (2014). GABA(A) receptor pi (GABRP) stimulates basal-like breast cancer cell migration through activation of extracellular-regulated kinase 1/2 (ERK1/2). The Journal of biological chemistry, 289(35), 24102â24113. https://doi.org/10.1074/jbc.M114.593582

Stierand, K., Maass, P. C., & Rarey, M. (2010). Drawing the PDB - Protein-Ligand Complexes in two Dimensions. Medicinal Chemistry Letters, 1(9), 540-545. https://doi.org/10.1021/ml100164p

Sung, H. Y., Yang, S. D., Ju, W., & Ahn, J. H. (2017). Aberrant epigenetic regulation of GABRP associates with aggressive phenotype of ovarian cancer. Experimental & molecular medicine, 49(5), e335. https://doi.org/10.1038/emm.2017.62

Swamidass S. J. (2011). Mining small-molecule screens to repurpose drugs. *Briefings in bioinformatics*, *12*(4), 327–335. https://doi.org/10.1093/bib/bbr028

Szklarczyk, D., Franceschini, A., Wyder, S., Forslund, K., Heller, D., Huerta-Cepas, J., Simonovic, M., Roth, A., Santos, A., Tsafou, K. P., Kuhn, M., Bork, P., Jensen, L. J., & von Mering, C. (2015). STRING v10: protein-protein interaction networks, integrated over the tree of life. *Nucleic acids research*, *43*(Database issue), D447–D452. https://doi.org/10.1093/nar/gku1003

Tanimura, S., Asato, K., Fujishiro, S. H., & Kohno, M. (2003). Specific blockade of the ERK pathway inhibits the invasiveness of tumor cells: down-regulation of matrix metalloproteinase-3/-9/-14 and CD44. *Biochemical and biophysical research communications*, *304*(4), 801–806. https://doi.org/10.1016/s0006-291x(03)00670-3

Tian, X., Ye, M., Zhang, R., Huo, Y., Wang, Y., Zhang, S., Ding, Y., & Zhang, X. (2012). GABA-A receptor modulators affect the ERK signaling pathway and the proliferation of Hep-2 cells. Journal of Cancer Research and Clinical Oncology, 138(11), 1947-1956. doi: 10.1007/s00432-012-1278-8. PMID: 22915381.

To, K. W., & Cho, W. C. S. (2022). Drug Repurposing for Cancer Therapy in the Era of Precision Medicine. *Current molecular pharmacology*, *15*(7), 895–903. https://doi.org/10.2174/1874467215666220214104530.

Trott, O., & Olson, A. J. (2010). AutoDock Vina: improving the speed and accuracy of docking with a new scoring function, efficient optimization, and multithreading. Journal of computational chemistry, 31(2), 455-461.

Vedam, V. A. Varahi[1]; Nuthalapati, Poojith[2]; Ghanta, Mohan Krishna[3,]; David, Darling Chellathai[4]; Vijayalakshmi, M.[5]; Potla, Krishna Murthy[6]; Mary, Y. Sheena[7]. Antiproliferative Effects of Olanzapine against MCF-7 Cells and Its Molecular Interactions with Survivin. International Journal of Nutrition, Pharmacology, Neurological Diseases 12(2):p 72-78, Apr–Jun 2022. | DOI: 10.4103/ijnpnd.IJNPND_82_21

Wang, Y., & Zeng, J. (2013). Predicting drug-target interactions using restricted Boltzmann machines. *Bioinformatics (Oxford, England)*, *29*(13), i126–i134. https://doi.org/10.1093/bioinformatics/btt234

Xiaocao Zhao, Xuejiao Zhang, Dengyong Liu, (2021) Collagen peptides and the related synthetic peptides: A review on improving skin health. Journal of Functional Foods. Volume 86, 104680. ISSN 1756-4646. https://doi.org/10.1016/j.jff.2021.104680.

Yang, M., & Brackenbury, W. J. (2013). Membrane potential and cancer progression. Frontiers in physiology, 4, 185. https://doi.org/10.3389/fphys.2013.00185

Yeo, M., Kim, D. K., Park, H. J., Cho, S. W., Cheong, J. Y., & Lee, K. J. (2008). Blockage of intracellular proton extrusion with proton extrusions with proton pump inhibitor induces apoptosis in gastric cancer. Cancer science, 99(1), 185. (Retraction published Yeo M, Kim DK, Park HJ, Cho SW, Cheong JY, Lee KJ. Cancer Sci. 2008 Jan;99(1):185)

Yeung TL, Leung CS, Wong KK, Samimi G, Thompson MS, Liu J, Zaid TM, Ghosh S, Birrer MJ, Mok SC. TGF-beta modulates ovarian cancer invasion by upregulating CAF-derived versican in the tumor microenvironment. Cancer Res. 2013;73(16):5016–28.

Zhai, M., Yang, Z., Zhang, C., Li, J., Jia, J., Zhou, L., Lu, R., Yao, Z., & Fu, Z. (2020). APN-mediated phosphorylation of BCKDK promotes hepatocellular carcinoma metastasis and proliferation via the ERK signaling pathway. *Cell death & disease*, *11*(5), 396. https://doi.org/10.1038/s41419-020-2610-1

SUPPLMENTARY INFO

Table 1. A list of the FDA approved drugs ranked based on their affinity to ANPEP, including the specific model of the compound and the heavy atoms.

drug	heavyAtoms	model	affinity
BACITRACIN	100	2_01	-23.99
GRAMICIDIN	82	3_01	-23.08
HISTRELIN	96	4_01	-21.5
EVEROLIMUS	68	3_01	-21.11
BREMELANOTIDE	74	2_01	-20.04
GOSERELIN	91	4_01	-20.04
LANREOTIDE	77	1_01	-19.15
GANIRELIX	112	3_01	-18.77
PASIREOTIDE	77	2_01	-18.64
OCTREOTIDE	71	4_01	-18.16
LEUPROLIDE	87	1_01	-18.11
PIMECROLIMUS	56	4_01	-17.51
OXYTOCIN	69	3_01	-17.2
AFAMELANOTIDE	118	4_01	-17.14
ICATIBANT	92	3_01	-16.97
CANDESARTAN_CILEXETIL	45	3_01	-15.46
ISAVUCONAZONIUM	51	4_01	-15.38
LAPATINIB	40	4_01	-15.23
OLMESARTAN_MEDOXOMIL	41	3_01	-15.01
EVEROLIMUS	68	1_30	-14.71
IMATINIB	37	1_01	-14.65
AZITHROMYCIN	52	1_01	-14.64
NETARSUDIL	34	3_01	-14.37
LEDIPASVIR	65	4_01	-14.33
ARGATROBAN	35	3_01	-14.24
IRBESARTAN	32	2_01	-14.22
FEDRATINIB	37	4_01	-14.13
NINTEDANIB	40	1_01	-14
BEROTRALSTAT	41	1_01	-13.91
PALIPERIDONE	31	3_01	-13.89
NERATINIB	40	4_01	-13.72
PALIPERIDONE_PALMITATE	48	2_01	-13.64
GRAMICIDIN	82	4_29	-13.64
AFATINIB	34	2_01	-13.56
OSIMERTINIB	37	2_01	-13.51
PAZOPANIB	31	1_01	-13.49

AXITINIB	28	2_01	-13.47
ILOPERIDONE	31	3_01	-13.4
AZELASTINE	27	1_01	-13.38
GLIPIZIDE	31	3_01	-13.35
NILOTINIB	39	2_01	-13.22
BOSUTINIB	36	3_01	-13.16
FEXOFENADINE	37	4_01	-13.14
ALISKIREN	39	4_01	-13.14
IVERMECTIN	62	4_01	-13.04
ABEMACICLIB	37	3_01	-13.01
KETOCONAZOLE	36	4_01	-12.95
OLAPARIB	32	1_01	-12.92
CARFILZOMIB	52	4_01	-12.92
ACALABRUTINIB	35	1_01	-12.91
CABOZANTINIB	37	3_01	-12.9
OLMESARTAN	33	2_01	-12.84
ABIRATERONE	26	1_01	-12.8
PEXIDARTINIB	29	1_01	-12.8
ITRACONAZOLE	49	2_01	-12.74
NETUPITANT	41	1_01	-12.73
GILTERITINIB	40	1_01	-12.68
BRIGATINIB	40	3_01	-12.54
IRINOTECAN	43	3_01	-12.49
GLASDEGIB	28	3_01	-12.47
LIFITEGRAST	41	4_01	-12.46
ISAVUCONAZOLE	31	3_01	-12.45
PALBOCICLIB	33	2_01	-12.45
CABERGOLINE	33	3_01	-12.37
PIMAVANSERIN	31	1_01	-12.36
LENVATINIB	30	4_01	-12.33
IVABRADINE	34	2_01	-12.32
BLEOMYCIN	96	1_01	-12.29
ALFENTANIL	30	1_01	-12.28
NICARDIPINE	35	1_01	-12.26
PARICALCITOL	30	3_01	-12.24
IBUTILIDE	26	1_01	-12.19
BUSPIRONE	28	4_01	-12.18
AVANAFIL	34	1_01	-12.1
FOSTAMATINIB	40	2_01	-12.1
CANDESARTAN_CILEXETIL	45	3_27	-12.1
NORELGESTROMIN	24	4_01	-12.09

PANOBINOSTAT	26	2_01	-12.08
LASMIDITAN	27	4_01	-12.08
AMIODARONE	31	2_01	-12.08
ACRIVASTINE	26	1_01	-12.04
GLYBURIDE	33	4_01	-11.98
OXICONAZOLE	26	4_01	-11.95
NEFAZODONE	33	1_01	-11.94
CALCITRIOL	30	2_01	-11.92
PIOGLITAZONE	25	2_01	-11.89
GLIMEPIRIDE	34	1_01	-11.89
IVOSIDENIB	41	3_01	-11.89
OXACILLIN	28	3_01	-11.81
ISRADIPINE	27	1_01	-11.8
IXABEPILONE	35	3_01	-11.8
BARICITINIB	26	4_01	-11.79
LAROTRECTINIB	31	4_01	-11.78
LABETALOL	24	2_01	-11.77
PENTAMIDINE	25	3_01	-11.74
OXYBUTYNIN	26	1_01	-11.74
ALMOTRIPTAN	23	1_01	-11.71
IDARUBICIN	36	2_01	-11.64
FAMOTIDINE	20	1_01	-11.59
PERAMPANEL	27	2_01	-11.59
OLOPATADINE	25	3_01	-11.56
GENTAMICIN	33	4_01	-11.55
GEFITINIB	31	1_01	-11.49
PALONOSETRON	22	4_01	-11.47
NIRAPARIB	24	2_01	-11.47
AVATROMBOPAG	42	3_01	-11.44
INDAPAMIDE	24	3_01	-11.41
IBRUTINIB	33	3_01	-11.36
NORGESTIMATE	27	1_01	-11.28
IMATINIB	37	3_27	-11.26
PIMOZIDE	34	1_01	-11.23
ARIPIPRAZOLE	30	1_01	-11.21
NILOTINIB	39	3_29	-11.19
ONDANSETRON	22	3_01	-11.18
BOSENTAN	39	3_01	-11.18
PACLITAXEL	62	4_01	-11.16
HYDROXYCHLOROQUINE	23	2_01	-11.14
BREXPIPRAZOLE	31	2_01	-11.13

FLURAZEPAM	27	1_01	-11.12
FORMOTEROL	25	3_01	-11.1
CALCIFEDIOL	29	3_01	-11.1
PAROXETINE	24	3_01	-11.08
CARVEDILOL	30	1_01	-11.08
IDELALISIB	31	3_01	-11.08
PIROXICAM	23	3_01	-11.05
OLMESARTAN_MEDOXOMIL	41	1_27	-11.05
BAZEDOXIFENE	35	4_01	-11.04
ACEBUTOLOL	24	2_01	-11.01
ARFORMOTEROL	25	3_01	-11.01
FLAVOXATE	29	2_01	-11
ALPELISIB	30	4_01	-11
AMITRIPTYLINE	21	2_01	-10.98
LEMBOREXANT	30	2_01	-10.93
BROMOCRIPTINE	43	1_01	-10.93
BRINZOLAMIDE	23	2_01	-10.89
ISOCARBOXAZID	17	3_01	-10.86
PERPHENAZINE	27	4_01	-10.83
AMISULPRIDE	25	3_01	-10.82
PANCURONIUM	41	1_01	-10.82
ALECTINIB	36	4_01	-10.78
ALOSETRON	22	1_01	-10.77
BUTENAFINE	24	3_01	-10.77
BEPOTASTINE	27	3_01	-10.77
BROMPHENIRAMINE	19	1_01	-10.75
ALOGLIPTIN	25	2_01	-10.73
CABAZITAXEL	60	1_01	-10.73
OLODATEROL	28	1_01	-10.67
ALPRAZOLAM	22	2_01	-10.66
BREMELANOTIDE	74	3_30	-10.66
BACITRACIN	100	2_30	-10.65
LETROZOLE	22	4_01	-10.63
ALCAFTADINE	23	4_01	-10.63
APALUTAMIDE	33	1_01	-10.63
BIMATOPROST	30	1_01	-10.58
PHENTOLAMINE	21	3_01	-10.56
BETAXOLOL	22	3_01	-10.52
BENZPHETAMINE	18	1_01	-10.47
FINGOLIMOD	22	4_01	-10.47
LATANOPROST	31	1_01	-10.47

HALOPERIDOL	26	4_01	-10.45
CANAGLIFLOZIN	31	4_01	-10.43
NORTRIPTYLINE	20	4_01	-10.41
ANASTROZOLE	22	2_01	-10.41
BINIMETINIB	27	4_01	-10.41
LEVOBETAXOLOL	22	4_01	-10.4
BICALUTAMIDE	29	3_01	-10.38
NIZATIDINE	21	3_01	-10.33
KETOTIFEN	22	2_01	-10.33
CABERGOLINE	33	4_27	-10.28
LAMOTRIGINE	16	1_01	-10.27
LEVAMLODIPINE	28	2_01	-10.25
FULVESTRANT	41	4_01	-10.24
NERATINIB	40	4_28	-10.23
LEVOBUNOLOL	21	1_01	-10.22
CARIPRAZINE	28	3_01	-10.21
PEMETREXED	31	3_01	-10.2
ABACAVIR	21	1_01	-10.18
ATOVAQUONE	26	3_01	-10.18
BELINOSTAT	22	1_01	-10.13
BISOPROLOL	23	1_01	-10.13
LEVOTHYROXINE	24	1_01	-10.13
LANSOPRAZOLE	25	3_01	-10.1
ACLIDINIUM	33	4_01	-10.1
PANTOPRAZOLE	26	4_01	-10.08
LAPATINIB	40	4_28	-10.08
IMIPRAMINE	21	2_01	-10.07
ASENAPINE	20	1_01	-10.04
CARTEOLOL	21	2_01	-10.04
FLUPHENAZINE	30	2_01	-10.03
BEROTRALSTAT	41	3_27	-10.01
AMOXAPINE	22	1_01	-10
FLUOXETINE	22	1_01	-9.996
PIMECROLIMUS	56	4_30	-9.994
AFATINIB	34	3_21	-9.993
GRANISETRON	23	3_01	-9.988
FENOLDOPAM	21	3_01	-9.986
FOSINOPRIL	39	4_01	-9.959
ABEMACICLIB	37	3_27	-9.947
ADAPALENE	31	1_01	-9.946
FEDRATINIB	37	1_26	-9.941

OSIMERTINIB	37	4_28	-9.932
ATOMOXETINE	19	2_01	-9.915
ATORVASTATIN	41	2_01	-9.909
NETARSUDIL	34	1_24	-9.907
CARBINOXAMINE	20	4_01	-9.901
APREPITANT	37	3_01	-9.9
AMCINONIDE	36	2_01	-9.892
ALVIMOPAN	31	2_01	-9.887
PALIPERIDONE_PALMITATE	48	1_27	-9.876
IVOSIDENIB	41	1_25	-9.858
HYDROCHLOROTHIAZIDE	17	3_01	-9.857
PHENIRAMINE	18	2_01	-9.843
APIXABAN	34	3_01	-9.834
GLIPIZIDE	31	1_30	-9.821
ATENOLOL	19	3_01	-9.792
LEDIPASVIR	65	1_26	-9.79
LEFLUNOMIDE	19	2_01	-9.778
OLANZAPINE	22	2_01	-9.767
HYDRALAZINE	12	4_01	-9.76
HISTRELIN	96	2_30	-9.749
APOMORPHINE	20	3_01	-9.742
ISAVUCONAZONIUM	51	4_29	-9.736
BARICITINIB	26	4_23	-9.714
EZETIMIBE	30	3_01	-9.713

Table 2. List of the FDA approved molecules suggested by connectivity map to reverse the genetic signature of the upregulated genes of Claudin Low Breast Cancer. (Summary of all cell lines)

SCORE	ID	NAME	DESCRIPTION
-99.93	BRD-K16508793	diazepam	Benzodiazepine receptor agonist
-99.82	BRD-K56614220	clofazimine	GK0582 inhibitor
-98.98	BRD-A22380646	Pantoprazole	ATPase inhibitor
-98.77	BRD-A29644307	nomifensine	Dopamine uptake inhibitor
-98.7	BRD-K32398298	alprazolam	Benzodiazepine receptor agonist
-98.63	BRD-M07438658	lapatinib	EGFR inhibitor
-98.45	BRD-K02130563	panobinostat	HDAC inhibitor
-98.38	BRD-K18895904	Olanzapine	Dopamine receptor antagonist
-97.96	BRD-K88560311	rucaparib	PARP inhibitor
-97.92	BRD-K19416115	sitagliptin	Dipeptidyl peptidase inhibitor
-96.55	BRD-A15297126	fluocinonide	Glucocorticoid receptor agonist
-96.37	BRD-A23637604	oxymetholone	Androgen receptor agonist
-96.31	BRD-K00532621	midazolam	Benzodiazepine receptor agonist
-96	BRD-K67174588	toremifene	Estrogen receptor antagonist
-95.43	BRD-A35108200	dexamethasone	Glucocorticoid receptor agonist
-95.42	BRD-K20285085	fostamatinib	SYK inhibitor
-95.23	BRD-A78391468	prednisolone	Glucocorticoid receptor agonist
-95.14	BRD-A33168282	sotalol	Adrenergic receptor antagonist
-95.03	BRD-A65280694	molindone	Dopamine receptor antagonist
-94.87	BRD-K28761384	zuclopenthixol	Dopamine receptor antagonist
-94.07	BRD-K51485625	ritonavir	HIV protease inhibitor
-94.05	BRD-K50388907	fenofibrate	PPAR receptor agonist
-93.76	BRD-K38003476	clocortolone	Glucocorticoid receptor agonist
-93.66	BRD-A62434282	goserelin	Gonadotropin releasing factor hormone receptor agonist
-93.66	BRD-K81709173	halcinonide	Glucocorticoid receptor agonist
-93.4	BRD-A83237092	fulvestrant	Estrogen receptor antagonist
-93.13	BRD-A67438293	treprostinil	Prostacyclin analog
-93.06	BRD-A07000685	hydrocortisone	Glucocorticoid receptor agonist
-92.46	BRD-A16754160	ampicillin	Bacterial cell wall synthesis inhibitor
-92.45	BRD-K95309561	dienestrol	Estrogen receptor agonist
-92.29	BRD-A54596827	solifenacin	Acetylcholine receptor antagonist
-92.11	BRD-A83892713	rifampicin	RNA polymerase inhibitor
-92.11	BRD-K13514097	everolimus	MTOR inhibitor
-91.65	BRD-K08924299	palonosetron	Serotonin receptor antagonist
-91.41	BRD-A51820102	econazole	Bacterial cell wall synthesis inhibitor
-91.16	BRD-K44094599	tacrolimus	Calcineurin inhibitor
-90.96	BRD-A14395271	mesoridazine	Dopamine receptor antagonist
-90.27	BRD-A79803969	memantine	Glutamate receptor antagonist

Table 3. List of the FDA approved molecules suggested by connectivity map to reverse the genetic signature of the upregulated genes of Claudin Low Breast Cancer. (MCF7 cell line)

SCORE	ID	NAME	DESCRIPTION
-99.98	BRD-A83892713	rifampicin	RNA polymerase inhibitor
-99.96	BRD-K19416115	sitagliptin	Dipeptidyl peptidase inhibitor
-99.95	BRD-K18895904	Olanzapine	Dopamine receptor antagonist
-99.94	BRD-K59456551	methotrexate	Dihydrofolate reductase inhibitor
-99.79	BRD-A91699651	chloroquine	Antimalarial
-99.73	BRD-K44876623	zolpidem	Benzodiazepine receptor agonist
-99.72	BRD-A02759312	betaxolol	Adrenergic receptor antagonist
-99.65	BRD-K44779798	miglitol	Glucosidase inhibitor
-99.64	BRD-A34751532	homosalate	HSP inducer
-99.57	BRD-K70778732	trazodone	Adrenergic receptor antagonist
-99.55	BRD-K51485625	ritonavir	HIV protease inhibitor
-99.5	BRD-K05926469	lenalidomide	Antineoplastic
-99.44	BRD-K13926615	vardenafil	Phosphodiesterase inhibitor
-99.34	BRD-K50938786	ropivacaine	Sodium channel blocker
-99.3	BRD-K11399644	phenformin	AMPK activator
-99.15	BRD-A90515964	guaifenesin	Expectorant
-99.04	BRD-K97810537	beclometasone	Glucocorticoid receptor agonist
-98.97	BRD-K27721098	clopidogrel	Purinergic receptor antagonist
-98.96	BRD-A90131694	alclometasone	Glucocorticoid receptor agonist
-98.9	BRD-A90799790	isradipine	Calcium channel blocker
-98.79	BRD-A62434282	goserelin	Gonadotropin releasing factor hormone receptor agonist
-98.72	BRD-A09533288	verapamil	Calcium channel blocker
-98.71	BRD-A67438293	treprostinil	Prostacyclin analog
-98.67	BRD-K80396088	gliquidone	Sulfonylurea
-98.65	BRD-K54416256	methimazole	Antithyroid
-98.58	BRD-K37798499	etoposide	Topoisomerase inhibitor
-98.31	BRD-K28761384	zuclopenthixol	Dopamine receptor antagonist
-98.14	BRD-A22256192	terazosin	Adrenergic receptor antagonist
-97.69	BRD-K00673382	famotidine	Histamine receptor antagonist
-97.66	BRD-A22380646	Pantoprazole	ATPase inhibitor
-97.51	BRD-K32830106	guanfacine	Adrenergic receptor agonist
-97.44	BRD-A94543220	bifonazole	Sterol demethylase inhibitor
-97.39	BRD-K61341215	vecuronium	Acetylcholine receptor antagonist
-97.28	BRD-K52080565	rilmenidine	Imidazoline receptor agonist
-96.96	BRD-K79254416	decitabine	DNA methyltransferase inhibitor
-96.76	BRD-A82371568	clofarabine	Ribonucleoside reductase inhibitor
-96.72	BRD-A44008656	doxylamine	Histamine receptor antagonist
-96.52	BRD-K74514084	pazopanib	KIT inhibitor

-96.51	BRD-M07438658	lapatinib	EGFR inhibitor
-96.35	BRD-K10852020	tolcapone	Catechol O methyltransferase inhibitor
-96.34	BRD-K35941380	methysergide	Serotonin receptor antagonist
-96.29	BRD-K91315211	betahistine	Histamine receptor agonist
-96.16	BRD-A65280694	molindone	Dopamine receptor antagonist
-95.92	BRD-M00539986	formoterol	Adrenergic receptor agonist
-95.84	BRD-K90789829	nefazodone	Adrenergic inhibitor
-95.24	BRD-K68132782	terbinafine	Fungal squalene epoxidase inhibitor
-94.91	BRD-A10715913	sulpiride	Dopamine receptor antagonist
-94.3	BRD-A20239487	atenolol	Adrenergic receptor antagonist
-92.69	BRD-A17448384	beclometasone	Glucocorticoid receptor agonist
-92.69	BRD-K36616567	doxepin	Histamine receptor antagonist
-92.45	BRD-K73978287	hydrocortisone	Glucocorticoid receptor agonist
-92.17	BRD-A65076780	dihydroergocristine	Adrenergic receptor antagonist
-92.08	BRD-A14395271	mesoridazine	Dopamine receptor antagonist
-91.77	BRD-K33211335	dextromethorphan	Glutamate receptor antagonist
-91.65	BRD-A61793559	metolazone	Carbonic anhydrase inhibitor
-91.22	BRD-K14965640	ibuprofen	Cyclooxygenase inhibitor
-91.21	BRD-M30523314	vinorelbine	Tubulin inhibitor
-91.16	BRD-A35912562	pregnenolone	Glutamate receptor modulator
-91.06	BRD-K50938287	sumatriptan	Serotonin receptor agonist
-91.02	BRD-K27184429	levocetirizine	Histamine receptor antagonist
-90.95	BRD-A62525898	prednisone	Glucocorticoid receptor agonist
-90.83	BRD-K12994359	valdecoxib	Cyclooxygenase inhibitor
-90.43	BRD-A97739905	ketoprofen	Cyclooxygenase inhibitor
-90.32	BRD-A99411506	esculin	Antioxidant
-90.18	BRD-K16508793	diazepam	Benzodiazepine receptor agonist
-90.16	BRD-K67977190	eprosartan	Angiotensin receptor antagonist